Zebrafish Tbx16 regulates intermediate mesoderm cell fate by attenuating Fgf activity

Rachel M. Warga[a,c], **Rachel L. Mueller**[b,c], **Robert K. Ho**[c], and **Donald A. Kane**[a]

[a]Department of Biological Sciences, Western Michigan University, Kalamazoo, MI 49008, USA

[b]Department of Biology, Colorado State University, Fort Collins CO 80523

[c]Department of Organismal Biology and Anatomy, University of Chicago, 1027 East 57th Street, Chicago, IL 60637

Abstract

Progenitors of the zebrafish pronephros, red blood and trunk endothelium all originate from the ventral mesoderm and often share lineage with one another, suggesting that their initial patterning is linked. Previous studies have shown that *spadetail* (*spt*) mutant embryos, defective in *tbx16* gene function, fail to produce red blood cells, but retain the normal number of endothelial and pronephric cells. We report here that *spt* mutants are deficient in all the types of early blood, have fewer endothelial cells as well as far more pronephric cells compared to wildtype. *In vivo* cell tracing experiments reveal that blood and endothelium originate in *spt* mutants almost exclusively from the dorsal mesoderm whereas, pronephros and tail originate from both dorsal and ventral mesoderm. Together these findings suggest possible defects in posterior patterning. In accord with this, gene expression analysis show that mesodermal derivatives within the trunk and tail of *spt* mutants have acquired more posterior identity. Secreted signaling molecules belonging to the Fgf, Wnt and Bmp families have been implicated as patterning factors of the posterior mesoderm. Further investigation demonstrate that Fgf and Wnt signaling are elevated throughout the nonaxial region of the *spt* gastrula. By manipulating Fgf signaling we show that Fgfs both promote pronephric fate and repress blood and endothelial fate. We conclude that Tbx16 plays an important role in regulating the balance of intermediate mesoderm fates by attenuating Fgf activity.

Keywords

Introduction

The kidneys, red blood and trunk endothelium are mesodermal derivatives that share a common developmental origin in the vertebrate embryo. In the model systems studied thus far, all three tissues derive from mesoderm on the ventral side of the gastrula, an area that tends to produce the posterior of the embryo (Delarue et al., 1994; Hatada and Stern, 1994; Kimmel et al., 1990; Lane and Sheets, 2006; Vogeli et al., 2006; Warga et al., 2009). In

Corresponding author: Rachel M. Warga, Department of Biological Sciences, Western Michigan University, Kalamazoo, MI 49008, USA, Phone: (269) 387-0781, rachel.warga@wmich.edu.

zebrafish, these three tissues frequently descend from the same blastula progenitor cell (Warga et al., 2009) and even once germ layers are established and the basic body plan is evident, they remain closely associated (reviewed in: (Davidson and Zon, 2004; Drummond, 2003). By the end of gastrulation, presumptive kidney, red blood and trunk endothelium reside in paired bands of tissue that we refer to here as intermediate mesoderm because it is sandwiched between paraxial mesoderm and lateral plate mesoderm all of which are distinguishable from each other by gene expression (Rohde et al., 2004). Ultimately intermediate mesoderm in the trunk segregates into a nephric portion that epithelializes into the paired pronephric kidneys and a blood/endothelial portion, which migrates medially to become the intermediate cell mass, a composite of blood cells and encapsulating endothelium that eventually form the blood vessels (reviewed in: (Davidson and Zon, 2004; Drummond, 2003).

How the intermediate mesoderm is patterned into the individual cell fates is still largely unclear. In amniotes as well as frogs and fishes, when the intermediate mesoderm can first be distinguished molecularly, all cells express genes involved in kidney development (Heller and Brändli, 1999; Pfeffer et al., 1998). Later, subsets of cells in the intermediate mesoderm begin to express additional genes more exclusive to a kidney or red blood/endothelial program of development, demarcating presumptive kidney cells from presumptive blood/endothelial cells. Eventually, cells in the red blood/endothelial field restrict to a red blood or endothelial-specific gene program (reviewed in: (Davidson and Zon, 2004; Dressler, 2006; Drummond, 2003). This progressive refinement in gene expression suggests that perhaps kidney fate is an intermediate step in the blood and endothelial differentiation pathway, which takes longer to be established. A similar phenomenon of hierarchy is likewise observed within the intermediate mesoderm lineages of zebrafish (Warga et al., 2009).

A number of signaling molecules are implicated in patterning the kidneys, red blood and endothelium. These signaling molecules include members of the Fgf and Wnt families, as well as members of the Bmp family (reviewed in: (Baron and Fraser, 2005; Chappell and Bautch, 2010; Dressler, 2009). In addition, Fgfs, Wnts and Bmps are essential during gastrulation for inducing and maintaining ventral mesoderm fate (reviewed in: (Kimelman, 2006; Schier and Talbot, 2005), which in general generates the more posterior mesodermal tissues (Kimmel et al., 1990; Lane and Sheets, 2006; Warga and Nusslein-Volhard, 1999). Other molecules critical for patterning the posterior mesoderm include T-box transcription factors, many of which interact with the Fgf, Wnt and Bmp signaling pathways (reviewed in: (Naiche et al., 2005).

In zebrafish, a number of T-box genes are thought to be involved in posterior mesoderm patterning, these include: *no tail* (*ntl*) *spadetail* (*spt*) and *tbx6-like* (formerly *tbx6*) (Griffin et al., 1998; Hug et al., 1997; Schulte-Merker et al., 1994). Only *spt* however, is known to have a role in blood, endothelial or kidney development. The product of *spt*, Tbx16, normally is required cell autonomously during gastrulation in the presumptive nonaxial mesoderm (Ho and Kane, 1990; Row et al., 2011). In its absence, mesodermal cells fail to activate muscle-specific genes or migrate correctly to the dorsal axis (Griffin and Kimelman, 2002; Kimmel et al., 1989; Row et al., 2011; Weinberg et al., 1995; Yamamoto et al., 1998). Rather, mutant cells locate to the tailbud and acquire new fates leaving the trunk noticeably deficient in muscle and the tail with a surplus of cells (Amacher et al., 2002; Kimmel et al., 1989). *spt* mutants also fail to form red blood cells (Kimmel et al., 1989; Oates et al., 2001; Thompson et al., 1998), not only because *spt* function is required cell autonomously for red blood-specific gene expression, but potential signals from trunk muscle also are critical as a niche for red blood to differentiate (Rohde et al., 2004). Previous reports however, show that other intermediate mesoderm derivatives, including blood derived from the head intermediate

mesoderm, develop normally in *spt* mutants (Kimmel et al., 1989; Le Guyader et al., 2007; Lieschke et al., 2002; Rohde et al., 2004; Thompson et al., 1998).

In a previous publication, we reported the elucidation of two intermediate mesoderm lineages (Warga et al., 2009). One that derives from the dorsal half of the gastrula, locates to the head and produces endothelium and macrophages (a type of white blood). The second derives from the ventral half of the gastrula, locates to the trunk and produces pronephros, endothelium and erythrocytes (red blood). In this study, two other blood types namely neutrophils (also a type of white blood) and platelets often derived from the lineage that included red blood cells. This result prompted us to ask if these associated cell types were also lacking in *spt* mutants. Here we report that all types of embryonic blood, including macrophages, are deficient in *spt* mutants. Furthermore, we show that *spt* function is not simply required for blood cell development, but that it correctly balances the proportion of blood, endothelium and kidney. Unexpectedly the underlying cause for this imbalance in tissues results from excess Fgf8a induced activity, which favors nephric fate over blood and endothelial fate.

Materials and Methods

Embryos, heat-shocks, antisense morpholino and chemical treatments

Fate mapping, *in situ* analysis, antisense morpholino and pharmacology were performed in embryos derived from crosses of identified *spt*[b104] heterozygotes.

To induce Fgf8a expression, we used embryos derived from heterozygous tg(hsp90l:fgf8a) (Hans et al., 2007) fish crossed to wildtype fish, resulting in 50% of the progeny carrying the transgene. All embryos, including those not carrying the transgene, were heat-shocked at 40°C for thirty minutes. A portion of these embryos were fixed an hour after heat-shock and probed for ubiquitous *fgf8a* expression to test reliability of induction as ectopic *fgf8a* mRNA is retained for approximately 2 hours after heat-shock (Hans et al., 2007). Genotype was determined by PCR using the following primers: *hspF*: 5′-CATGTGGACTGCCTATGTTCATCT-3′ and *fgf8aR*: 5′-TGTCCATGAAGGTGAGGAGCGCAGC-3′, which produces a 650 bp product in embryos carrying the transgene.

To block Fgf8a expression, we used a morpholino against *fgf8a*, covering the translational start codon 5′ - GAGTCTCATGTTTATAGCCTCAGTA - 3′ (Araki and Brand, 2001). We injected between 2–5 ng of morpholino per embryo at the one- to eight-cell stage. Between 4–5 ng produces a phenotype that phenocopies the *acerebellar* (*ace*) mutant phenotype, a known loss-of-function in *fgf8a* (Araki and Brand, 2001; Reifers et al., 1998).

To Block Fgf receptor activity, embryos were treated for one hour with the Fgf receptor inhibitor SU5402 (Tocris Bioscience) at 25 μM. We tested a number of concentrations and found this concentration caused the least developmental defects in wild-type embryos. Blocking Fgf receptor activity for one hour rather than continuous treatment of lower concentrations as performed in other studies (Griffin and Kimelman, 2003) more accurately phenocopied the *ace* mutant.

All Fgf experiments were monitored using the midbrain-hindbrain boundary and/or the otic vesicle as an internal control for Fgf8a induced activity. Both are visualized by *pax2a* expression (Pfeffer et al., 1998) and depend upon Fgf8a signaling for their induction or maintenance (Hans et al., 2007; Phillips et al., 2001; Reifers et al., 1998). Overexpressing Fgf8a during gastrulation decreases the size of the otic vesicle (Hans et. al. 2007), whereas

loss of Fgf8a function causes the midbrain-hindbrain boundary to diminish and eventually disappear following its seemingly normal induction (Reifers et. al. 1998).

Exogenous RA was provided by treating embryos for one hour with 1 μm RA (Sigma-Aldrich) following the protocol by Stafford and Prince (2002).

in situ hybridization, antibody staining and cell counting

Whole-mount RNA *in situ* hybridization was carried out using digoxigenin-labeled riboprobes following the protocol in (Thisse and Thisse, 2008). Whole-mount antibody staining was carried out using an anti-β-catenin antibody (Sigma-Aldrich) followed by detection with the Vectastain Elite ABC peroxidase kit (Vector laboratories) and a DAB enzyme substrate reaction.

Cell counts of intermediate mesoderm tissues, were done by mounting embryos dorsal up and counting all the cells in an individual stripe at 200x magnification on a Zeiss Axiophot or Zeiss Axioskop. By focusing up and down through several planes and moving the field as necessary we were able to distinguish all the cells in an individual stripe marked by a particular riboprobe. Cell counts were frequently done more than once producing similar counts, validating this method of quantification. As a further test of the data collected by cell counts, we compared our data for the different intermediate mesoderm fates in Fig. 2 to data collected by performing gene set enrichment analysis for tissue-specific genes included in the supplementary data. Both are in agreement with each other, again demonstrating that counting cells is reliably accurate.

Lineage tracing and fate map construction

Lineage tracing and fate map construction were performed as described in Warga, et al. (2009). The entire data set included 155 wild-type clones, and 50 mutant clones (Supplementary Fig. 1).

Gene set enrichment and individual gene analysis

Gene set enrichment analysis was applied to previously published microarray data derived from wildtype and sibling *spt* mutants collected at the 4/5-somites (~11.5 hours) and 21-somites (19.5 hours) (Mueller et al., 2010). Gene sets were compiled from the following sources: the ZFIN anatomical ontology browser (http://zfin.org), the gene ontology information in the Affymetrix zebrafish array annotation, and the literature. Gene sets (listed in supplemental data) included 32 red blood genes, 21 white blood genes, 63 pronephric genes, and 22 endothelium genes. Affymetrix. CEL files for the two developmental stages were combined for enrichment analysis of each tissue type using the Expression File Creator module of the GenePattern software package (quantile normalization = yes, background correct = yes). Gene set enrichment analysis for the four tissues was run using GSEA software (http://www.broad.mit.edu/gsea/) at the probe level (Collapse dataset to gene symbols = False) with 1,000 gene set permutations. Eight genes were expressed in more than one tissue. Because inclusion of genes in multiple gene sets can affect statistical significance levels, analyses were repeated both including and excluding these eight genes.

Individual fold changes for *fgf8a*, *spry2* and *bon* expression were determined using the previously published microarray data derived from control and sibling *tbx16*-deficient embryos collected at 75% epiboly (8 hours) (Garnett et al., 2009).

Results

spt mutants have a shortage of all types of embryonic blood

spadetail (*spt*) mutant embryos, lack red blood cells (erythrocytes) (Kimmel et al., 1989; Oates et al., 1999; Rohde et al., 2004; Thompson et al., 1998). Because we previously showed that neutrophils (a type of white blood) and platelets derive from red blood lineages (Warga et al., 2009), we postulated that these other types of blood might be missing as well in *spt* mutants. To investigate this possibility we examined a variety of blood-specific genes in the intermediate cell mass at approximately the 21-somite stage (19.5 hours; Fig. 1 and Supplementary Fig. 2A–C). These included genes encoding transcriptional regulators important for all early blood (*tal1*, *drl* and *lmo2* (Herbomel et al., 1999; Liao et al., 1998; Thompson et al., 1998) as well as genes specific only to red blood cells such as the GATA transcription factor *gata1* and the hemoglobin *hbbe2* (Brownlie et al., 2003; Detrich et al., 1995) or genes specific only to white blood cells such as the ETS-domain transcription factor *spi1* and the peroxidase enzyme *mpo* (Bennett et al., 2001; Lieschke et al., 2001; Lieschke et al., 2002), including the actin binding protein *lcp* expressed only in early macrophages (Herbomel et al., 1999), a cell type that is not derived from the red blood lineage (Warga et al., 2009). Without exception, many fewer cells expressed each of these markers in *spt* mutants indicating that blood in general, rather than red blood in particular, is deficient in *spt* mutants.

spt mutants have more pronephros and slightly less endothelium

Previous studies reported that the kidney and endothelium are disorganized, but retain their normal cell quantities in *spt* mutants (Oates et al., 1999; Rohde et al., 2004; Thompson et al., 1998). We saw similar disorganization, but found that *spt* mutants had many more pronephric precursors, and fewer trunk endothelial precursors than wildtype. At the 11-somite stage (14.5 hours), the paired-box transcription factor *pax2a* is normally expressed throughout the entire nephric portion of the intermediate mesoderm, whereas the Notch ligand *jag2*, at this time, is expressed in just the anterior part (Krauss et al., 1991; Ma and Jiang, 2007; Pfeffer et al., 1998). In *spt* mutants, stripes of *pax2a* expression were broader and *jag2* expression reached further caudal (Fig. 2A, B). Likewise at this time, the proto-oncogene *fli1a* and endothelial cell adhesion molecule *cdh5* are normally expressed throughout the entire endothelial portion of the intermediate mesoderm (Larson et al., 2004; Thompson et al., 1998). In *spt* mutants, stripes of *fli1a* and *cdh5* expression in the trunk were disordered and patchy (Fig. 2C, D). To quantify these observations we counted the number of cells marked by these various genes at 14.5 hours. Mutant embryos had approximately one third more kidney precursors, and slightly less endothelial precursors than wildtype (Fig. 2J). By comparison, the number of cells in the mutant that expressed the blood transcriptional regulators *spi1, gata1,* and *tal1* were greatly reduced compared to normal (Fig. 2E–G, J), showing that in the trunk, mutants have few blood precursors at 14.5 hours, red or white.

Most of the intermediate mesoderm is located in the trunk, however a portion does reside in the head. This population of cells do not share lineage with red blood (Warga et al., 2009) and only produces endothelium or macrophages (also white blood) (Herbomel et al., 1999). Here at 14.5 hours, the shortage of blood precursors was less severe and the number of endothelial progenitors was normal (Fig. 2H, I, K and data not shown). Thus some intermediate mesoderm tissues in the mutant are largely unchanged.

To further test if more cells are allocated to kidney and less to blood and endothelium in *spt* mutants, we performed gene set enrichment analysis on our previously published microarray data collected at ~11.5 hours and 19.5 hours (Mueller et al., 2010). Consistent with previous

reports, as well as our current results that mutants have fewer erythrocytes, the red blood gene set was significantly downregulated in *spt* mutant tissue relative to wild-type tissue (False Discovery Rate q-value < 0.001, normalized enrichment score = −2.99). In agreement with our *in situ* analysis, the white blood gene set was also downregulated in *spt* mutant tissue relative to wild-type tissue (False Discovery Rate q-value = 0.022, normalized enrichment score = −1.61) while the nephric gene set was significantly upregulated (False Discovery Rate q-value = 0.002, normalized enrichment score = 1.77). The endothelial gene set did not appear significantly enriched in either genotype (False Discovery Rate q-value > 0.5), which may reflect the much smaller difference between mutant and wildtype observed above. Eight of the genes we analyzed were expressed in two tissue categories; therefore we reran the data with their exclusion and obtained similar results (False Discovery Rate q-values: q < 0.001, q = 0.1, q = 0.003, and q > 0.5 for red blood, white blood, kidney and endothelium, respectively). Together these experiments support our finding that *spt* mutants have more pronephros, much less blood and slightly less endothelium.

Altered morphogenesis of the *spt* trunk intermediate mesoderm

Presumptive trunk intermediate mesoderm first becomes apparent in the zebrafish during gastrulation (80% epiboly, 8.5 hours) upon transcription of the nephric marker *pax8*, a paralog of the paired-box transcription factor *pax2a* (Heller and Brändli, 1999; Pfeffer et al., 1998). Subsequently at the end of gastrulation (tailbud, 10 hours), all *pax8*-positive cells begin to co-express the nephric marker *pax2a*. Simultaneously, a subset of *pax8*-positive cells also begin to transcribe the endothelial marker *fli1a* and shortly later, the hematopoietic markers *tal1* and *lmo2* (Davidson et al., 2003; Walmsley et al., 2002). Thereafter a sequential activation of genes important for kidney, endothelial or blood cell fate appear, but by the 5-somite stage (11.7 hours), just after onset of expression of the first red blood-specific gene (*gata1*), populations of cells in the intermediate mesoderm seem to have limited their expression to genes specific for one particular fate (reviewed in (Davidson et al., 2003).

We investigated this spatiotemporal pattern of gene expression refinement in *spt* mutants. In general, all nephric and endothelial genes appeared on schedule, but all hematopoietic genes were severely delayed (Fig. 3A). Furthermore, from the onset, the spatial pattern of different cell fates was aberrant in *spt* mutants. Not only were nephric stripes closer together (likely due to the absence of trunk paraxial mesoderm) these stripes were wider and missing the most posterior portion (Fig. 3B). The same was true of endothelial stripes, although their spatial distribution was also patchier, suggesting a dearth of cells (Fig. 3C). Once they appeared, the few cells forming the blood stripes were even closer together and scattered within the intermediate mesoderm (Fig. 3D). We conclude that, not only does intermediate mesoderm not form in the proper place in *spt* mutants, but that once it forms, fewer cells switch over to an endothelial cell fate and far fewer cells to a blood cell fate.

Trunk intermediate mesoderm and tail map more dorsally and animally in *spt* mutants

Derivatives of the trunk intermediate mesoderm normally originate from the more ventral side of the gastrula close to the margin (Warga et al., 2009). We investigated where they derived in *spt* mutants by labeling single marginal cells of the blastula (3.5 hours) with lineage tracer dye and determining the location of the ensuing clone of cells at the onset of gastrulation (6 hours), before the majority of morphogenetic movements begin. Cell fate of these clones was subsequently ascertained at one to two days of development (Fig. 4A–E). In general, we found that the trunk intermediate mesoderm in *spt* mutants mapped more dorsally and more animally than in wildtype. Pronephros now derived from both the dorsal and ventral side (Fig. 4F), whereas blood (erythrocytes, neutrophils, and platelets), derived almost exclusively from the dorsal side (Fig. 4G). Though more subtle, this was true for

trunk endothelium as well (Fig. 4H). Furthermore unlike wildtype, the vast majority of trunk intermediate mesoderm clones mapped more than a cell diameter from the margin. The frequency of labeling intermediate mesoderm in *spt* mutants was about normal (60% versus 62%), but if one considered individual fates (as a proportion of all the intermediate mesoderm clones), there were notable differences between mutant and wildtype. Endothelial clones were about as frequent if trunk and head were considered together, however pronephric clones were twice as frequent in *spt* mutants and trunk blood clones half as frequent (Fig. 4J).

The *spt* intermediate mesoderm fate map suggests possible defects in anterior-posterior patterning as ventral mesoderm, not dorsal mesoderm, normally produces tissues found more posterior in the embryo (Kimmel et al., 1990; Lane and Sheets, 2006) and as a rule, the further a mesodermal cell is from the margin at the onset of gastrulation, the more posterior in the embryo its derivatives lie due to morphogenesis (Warga and Kimmel, 1990; Warga and Nusslein-Volhard, 1999). We tested this by mapping the origin of cells in the "spade tail", a hallmark feature of the mutant due to an abnormal accumulation of cells in the tailbud (Kimmel et al., 1989). For this we used the two most common tail derivatives: caudal fin mesenchyme and tail muscle. Normally these tissues derive exclusively from the most ventral cells of the gastrula (Warga and Nusslein-Volhard, 1999). In *spt* mutants, they derived from more dorsal and more animal locations (Fig. 4I), from cells that normally produce muscle in the trunk (Warga and Nusslein-Volhard, 1999). We conclude from this result that tail-specific fates in the *spt* gastrula have expanded into the trunk territory.

We also investigated where head intermediate mesoderm mapped in *spt* mutants. Normally this derives from the more dorsal side of the gastrula (Warga et al., 2009). However, in *spt* mutants, head endothelium and macrophages now also mapped ventrally (Fig. 4G, H), as has been found previously for other dorsally-derived fates in *spt* mutants (Kimmel et al., 1989; Warga and Nusslein-volhard, 1998) perhaps because cells in the *spt* organizer field do not cohere together properly behaving instead like cells more ventrally (Warga and Nusslein-volhard, 1998). While macrophage clones were somewhat more frequent in *spt* mutants (Fig. 4J), they only originated from clones at the margin (Fig. 4G) showing again that the normal axes (animal-vegetal and dorsal-ventral) that determine later anterior-posterior position are distorted in *spt* gastrulae.

Anterior-posterior patterning is altered in *spt* mutants

We next asked whether posterior tissue is overrepresented in *spt* mutants. In animals, *hox* genes confer regional identity to the developing embryo (Krumlauf 1994) and similar to their tetrapod counterparts, zebrafish hox genes display colinear expression along the anterior-posterior axis (Prince et al., 1998). All the posterior *hox* genes that we examined in the posterior mesoderm of *spt* mutants appeared to be more highly expressed (Fig. 5A–D and data not shown). At 15-somites (16.5 hours), strong expression of *hoxb6a* and *hoxb7a* in the mutant tailbud, was more extensive. This could simply reflect more cells in the mutant tailbud, however later expression at 18-somites (18 hours) of other *hox* genes such as *hoxd13a* in the presumptive cloaca and *hoxb8a* and *hoxc11b* in the presumptive pronephros, showed that once cells left the mutant tailbud and began to differentiate, not only were these genes expressed in far more cells, but also in cells rostral of their normal domains. This was particularly evident for *hoxb8a*, whose pronephric expression domain drastically shifted rostral up the trunk, suggesting that anterior cells in the *spt* mutant take on a more posterior fate.

The pronephros is the only intermediate mesoderm-derived tissue known to possess regional identity (Serluca and Fishman, 2001; Wingert et al., 2007). Examination of this tissue in more detail at 20-somites (19 hours), showed that genes specifically marking anterior kidney

segments such as the Wilms' Tumor suppressor gene *wt1a* (Serluca and Fishman, 2001) and the glutathione peptide biosynthesis enzyme *gss* (Thisse et al., 2001), were expressed in far fewer cells of the *spt* mutant (Fig. 5E, F). Whereas genes specifically marking posterior kidney segments such as *jag2* and *pax2a,* which at this time are now expressed caudally in the pronephric duct, were expressed in significantly more cells including many rostral of their normal domains (Fig. 5G, H). These changes of expression patterns in the kidney provide further support that anterior mesoderm is transfating to a more posterior fate in the mutant.

The Fgf and Wnt pathways are overactive in *spt* mutant gastrula

In vertebrates, the three most important signaling pathways which confer posterior identity to the embryo are Fgf, Wnt and Bmp (reviewed in: (Auleha and Pourquié, 2010; Diez del Corral and Storey, 2004; Stern et al., 2006). In zebrafish, components of each pathway are expressed during gastrulation (reviewed in: (Kimelman, 2006; Schier and Talbot, 2005), and this is the period when defects in *spt* mutants first appear (Ho and Kane, 1990; Kimmel et al., 1989; Rohde et al., 2004; Warga and Nusslein-volhard, 1998; Weinberg et al., 1995; Yamamoto et al., 1998). We first investigated Fgf signaling and found that the expression domain of *fgf8a*, a zebrafish ortholog of mouse, chick and frog *Fgf8* and the principle Fgf ligand involved in posterior fate (Draper et al., 2003; Ota et al., 2009; Reifers et al., 1998), appeared noticeably expanded on the ventral and lateral sides of *spt* mutants an hour after the onset of gastrulation (7 hours; Fig. 6A). Furthermore, expression in these territories appeared more robust in the mutant. Whether or not more cells express *fgf8a* at this time or the same numbers of cells express higher levels of *fgf8a,* analysis of published microarray results (Garnett et al., 2009) confirmed that *fgf8a* expression is upregulated 1.5-fold at 8 hours in *tbx16*-deficient embryos. In agreement with these results, later expression of *fgf8a* at the end of gastrulation (10 hours) in the mutant was also significantly more widespread and robust caudally and as the tailbud formed (11 hours), more cells than normal in the posterior of the embryo appeared to express high levels of *fgf8a*. We conclude from these results that *fgf8a* expression is elevated in *spt* mutants and that likely Fgf signaling is not normal.

We confirmed this by looking more closely at the Fgf and Wnt signaling pathway. The T-box transcription factor *no tail* (*ntl*), a zebrafish ortholog of mouse Brachyury (Schulte-Merker et al., 1994) is an immediate target of Fgf signaling (Draper et al., 2003; Griffin et al., 1995; Schulte-Merker and Smith, 1995). We found that the domain of *ntl* expression at 7 hours likewise was more extensive on the ventral side of *spt* gastrulae (Fig. 6B). Correspondingly later, there were also many more *ntl*-positive cells in mutants caudally. Oddly, like *fgf8a*, *ntl* expression dorsally at 7 hours was weaker than normal, even though later, *spt* mutants posses more notochord cells (Warga and Nusslein-volhard, 1998). Ntl regulates canonical Wnt signaling during gastrulation (Martin and Kimelman, 2008; Morley et al., 2009); akin to *fgf8a* and *ntl*, but more subtle, the expression domain of *wnt8a,* a zebrafish ortholog of mouse, chick and frog *Wnt8* and one of the principle Wnt ligands involved in posterior fate (Kelly et al., 1995; Lekven et al., 2001; Ramel et al., 2005), also appeared to be more extensive ventrally and laterally at 7 hours, as well as perhaps a bit more robustly expressed in these regions. This increased expression was more evident later at 10 and 11 hours in the posterior of the embryo (Fig. 6C). We also examined expression of the caudal identity transcription factors, *cdx4* and *cdx1a* (Davidson et al., 2003; Davidson and Zon, 2006)*,* which impart posterior identity by directly regulating *hox* gene function (reviewed in: (Lohnes, 2003). *cdx* genes are known to be regulated by Ntl (Garnett et al., 2009; Morley et al., 2009) and to be targets of Fgf and Wnt signaling (reviewed in: (Lohnes, 2003). In agreement with all our other observations, the expression domains of both *cdx4* and *cdx1a* appeared to be expanded on the ventral side of *spt* gastrula and likewise later

caudally in the embryo including abnormally strong expression in the intermediate mesoderm (Fig. 6D and E). This latter observation could perhaps explain the altered anterior-posterior patterning seen in the kidney (Fig. 5E–H) for *cdx4* overexpression in the nervous system promotes more posterior fate and interferes with more anterior fate (Skromne et al., 2007).

Members of the Sprouty family (*spry*) and Interleukin 17 receptor D (*il17rd*) encode intracellular regulators of receptor tyrosine kinase signaling that antagonize Fgf signal transduction (Fürthauer et al., 2002; Fürthauer et al., 2001; Fürthauer et al., 2004; Hacohen et al., 1998; Tsang et al., 2002). We investigated these as well as their expression is induced by Fgf8a (Fürthauer et al., 2002; Fürthauer et al., 2001; Tsang et al., 2002). As expected from *fgf8a* expression, *spry4* and *il17rd* were more highly expressed caudally in the *spt* mutant (Fig. 7A, B). Surprisingly, *spry2* was not (Fig. 7C). Although expression of *spry2* in the midbrain and hindbrain of the *spt* mutant seemed more robust (like *fgf8a*), in the posterior of the embryo, where *tbx16* is normally expressed (Griffin et al., 1998; Ruvinsky et al., 1998) *spry2* expression looked no different than wildtype. This result suggests that perhaps *spry2* is a downstream target of Tbx16 and analysis of the published 8 hour microarray (Garnett et al., 2009) indicates that *spry2* expression is downregulated 1.5-fold in *tbx16*-deficient embryos. Being that Spry2 is a negative regulator, when its function is compromised Fgf signal transduction becomes more intense and longer in duration (García-Domínguez et al., 2011).

We also looked in more detail at canonical Wnt signal transduction in *spt* mutants because previously, we noted that β-catenin was not located properly at the cortex of *spt* mutant cells (Warga and Nusslein-volhard, 1998). β-catenin, which has a function in cell adhesion, is also a transcriptional effector of canonical Wnt signaling. When Wnt signaling is active, levels of β-catenin build up in the cytosol, allowing it to enter the nucleus and activate transcription of target genes (Amin and Vincan, 2012; Schneider et al., 1996; Sylvie et al., 2011; van Amerongen and Nusse, 2009; Widelitz, 2005). Reinvestigation suggested that ventral mesoderm cells of the *spt* gastrula, which are less coherent with one another than wild-type cells (Warga and Nusslein-volhard, 1998), have more cytoplasmic and nuclear β-catenin than normal (Fig. 7D). This observation is consistent with a previous analysis indicating that Wnt signaling is highly upregulated in *spt* mutants during later blood development (Mueller et al., 2010). In sum, our results show that Fgf signaling is more active in the *spt* gastrula and likely Wnt signaling as well.

On the other hand, Bmp signaling seemed normal during gastrulation in the *spt* mutant. *bmp2b* and *bmp4*, two of the principle ligands involved in this pathway (Schier and Talbot, 2005) showed no changes in expression at 7 hours (Fig. 6F and data not shown). It was only once cells began to accumulate in the mutant tailbud that their expression domains increased. We also looked at the Bmp signal antagonist *chordin*, expressed in the organizer (Miller-Bertoglio et al., 1997). Here fewer cells in the prechordal plate of the mutant appeared to express *chordin* at 7 hours (Fig. 6G), however the prechordal plate of *spt* mutants is misshapen (Muyskens and Kimmel, 2007) not smaller (Warga and Nusslein-volhard, 1998). This is unlikely to alter the balance of Bmp signals and later *chordin* expression in *spt* mutants appeared relatively normal.

Other pathways that regulate posterior development, include RA (Diez del Corral and Storey, 2004; Duester, 2008; Stern et al., 2006) and noncanonical Wnt signaling (Agathon et al., 2003; Marlow et al., 2004; Pyati et al., 2005). Not surprisingly, we found defects in the RA pathway as early as gastrulation. This is because *aldh1a2* (also known as *raldh2*), encoding the enzyme necessary for the final metabolic step in retinoic acid synthesis is expressed in the paraxial mesoderm (Begemann et al., 2001). As paraxial mesoderm is not

specified properly in *spt* mutants (Griffin and Kimelman, 2002; Weinberg et al., 1995; Yamamoto et al., 1998) and its later derivative the somites are absent (Kimmel et al., 1989), few cells express *aldh1a2* at 7 hours (Fig. 6H). Between 10 and 11 hours during which time the first trunk somites form, *aldh1a2* expression was nearly gone in agreement with other studies (Gibert et al., 2006; Mueller et al., 2010). With respect to noncanonical Wnt signaling, expression of the noncanonical *wnt5b* ligand, also required for tail development (Marlow et al., 2004; Rauch et al., 1997), seemed normal at 7 hours (Fig. 6I) but, by 10 and 11 hours strong expression in the tailbud was more extensive and weaker expression in the paraxial mesoderm was highly reduced. We conclude that once posterior patterning is altered in the mutant due to excess Fgf signaling, other signaling pathways reflect this change in patterning.

Fgf signaling helps balance the ratio of intermediate mesoderm fates

It has been reported in zebrafish, that transient overexpression of *wnt8a* during gastrulation posteriorizes the intermediate mesoderm, resulting in more pronephric cells (Ueno et al., 2007). This study did not examine the effect on trunk blood or endothelium. To determine if transient overexpression of *fgf8a* had a similar effect on pronephric precursors and whether there was a critical time that overexpression had a greater effect, we repeated these experiments only with heat-shock-inducible Fgf8a transgenic embryos (Hans et al., 2007). Like the Wnt8a study, we heat-shocked for 30 minutes at the onset of gastrulation (6 hours), mid gastrulation (7.5 hours) and late gastrulation (9 hours), fixed them at early somite stages after one can unambiguously label all three tissues of the intermediate mesoderm (Davidson et al., 2003) and assayed for the number of cells allocated to pronephric fate by *pax2a* expression. We did not perform heat-shocks prior to gastrulation because it is well known that Fgf8 signaling patterns the mesoderm along the dorsal-ventral axis during pregastrulation stages by promoting dorsal and lateral mesodermal fates (Amaya et al., 1991; Fürthauer et al., 1997; Fürthauer et al., 2004) nor do *spt* mutants exhibit changes in *fgf8a* expression until after the onset of gastrulation (Fig. 6A).

We found that overexpression of *fgf8a* upon heat-shock at 6 hours, caused a significant increase in the number of pronephric precursors expressing *pax2a* at 6-somites (12 hours; compare Fig. 8A and 8B to 8C), whilst overexpression of *fgf8a* upon heat-shock at 7.5 hours or 9 hours, caused less of an effect or almost no effect on the number of pronephric cells (Fig. 8G). This was similar to the results obtained by overexpressing *wnt8a* (Ueno et al., 2007). On the other hand, overexpression of *fgf8a* at 6 hours resulted in a significant decrease in the number of red blood precursors expressing *gata1* as well as a minor decrease in the number of trunk endothelial precursors expressing *fli1a* (Fig. 8D–G and data not shown). Thus overexpression of *fgf8a* at 6 hours causes an intermediate mesoderm phenotype similar to that of the *spt* mutant that may be due to posteriorizing the intermediate mesoderm.

Studies have demonstrated that RA administered during gastrulation is also a posteriorizing factor (Hans and Westerfield, 2007; Hill et al., 1995; Kessel and Gruss, 1991; Kudoh et al., 2002; Phillips et al., 2001; Stafford and Prince, 2002), however it is also known to attenuate Fgf signaling by repressing *fgf8* transcription and/or accelerating its decay during early somite stages (Diez del Corral et al., 2003; Dubrulle and Pourquié, 2004). To delineate the effect of Fgf activity on the intermediate mesoderm and whether this is the consequence of changes in RA synthesis in the *spt* mutant due to decreased *aldh1a2* expression (Fig. 6H) we treated embryos for one hour with 1 μM RA at 6 hours, when overexpression of *fgf8a* had the greatest effect. Like overexpression of *fgf8a* at 6 hours, ectopic RA at this time resulted in more pronephric precursors and less red blood precursors, even in *spt* mutants (Supplementary Fig. 3), supporting the idea that the shift in blood, endothelial and kidney

cell fate is a consequence of too much posteriorizing activity. Furthermore, because ectopic RA had the same effect as overexpressing *fgf8a*, it is unlikely that increased *fgf8a* expression during gastrulation in the *spt* mutant or the changes in distribution of blood, endothelium and kidney stem from decreased RA levels.

We next asked what would happen if we interfered with Fgf8a activity. First we used an antisense morpholino against *fgf8a* that efficiently phenocopies the *acerebellar* (*ace*) mutant (Araki and Brand, 2001) a loss-of-function mutation in *fgf8a* (Reifers et al., 1998) and next we used SU5402, a chemical antagonist of the Fgf receptor (Mohammadi et al., 1997; Poss et al., 2000). Both gave similar phenotypes. Injection of 2–5 ng of *fgf8a* morpholino per embryo or treatment for one hour with 25 μM SU5402 at 6 hours (the critical time for Fgf8a overexpression) resulted in minimal alterations to morphology (in wildtype), but markedly fewer pronephric precursors at 12 hours (Fig. 8H, J, L and N). In wildtype, this was a 19% reduction, but in mutants, this was a 41% reduction likely because *spt* mutants are hypersensitive to inhibition of Fgf signaling (Griffin and Kimelman, 2003). We also treated embryos with SU5402 at later stages, but like overexpression of Fgf8a this had less of an effect. Knocking down Fgf8a function or interfering with Fgf signaling turned the spadetail of the mutant into a wildtype tailbud (Fig. 8O–T) and rescued the posterior patterning defects seen in the kidney of older mutant embryos (data not shown) supporting a causal relationship between posteriorization due to excessive Fgf8a and more pronephric precursors.

Notably, interfering with Fgf8a activity had an opposite effect on trunk blood (Fig. 8I, K, M and N). Injection of approximately 2–3 ng of *fgf8a* morpholino, which creates embryos that do not display the full *ace* phenotype, or treatment with SU5402 resulted in substantially more red blood precursors in wild-type embryos at 12 hours. However higher amounts of *fgf8a* morpholino (4–5 ng) that mimic the *ace* phenotype resulted in less blood progenitors suggesting that blood patterning is exquisitely sensitive to *fgf8a* levels. In contrast, most mutant embryos, either injected with the morpholino or treated with SU5402, showed no increase in the number of red blood precursors other than a few mutants treated with SU5402 (4/42). We obtained similar results assaying with a more universal blood marker *tal1* (Supplementary Fig. 4A). Hence simply decreasing Fgf8a signaling in *spt* mutants is not sufficient to restore trunk-derived blood, even though it increases head-derived blood (Supplementary Fig. 4C). Decreasing Fgf8a signaling, like increasing it, reduced the number of trunk endothelial precursors (Fig. 8N, supplementary Fig. 4B). Nevertheless, treated embryos always had more trunk endothelial cells than pronephric cells, which is not normally the case in the mutant. Thus lowering Fgf8a activity in *spt* mutants causes the ratio of cell types derived from the trunk intermediate mesoderm to more closely approximate the wild-type ratio (compare *spt* experiment to wild-type control in Fig. 8N). We conclude that elevated Fgf8a activity promotes kidney specification and represses blood specification whereas decreasing its activity has the opposite effect. On the other hand, both increased and decreased Fgf8a activity has a similar effect on endothelial specification that is somewhat inhibitory.

Discussion

This study reveals a previously uncharacterized role for *spt* function in intermediate mesoderm patterning. While previous studies showed that *spt* mutants lacked red blood, our work demonstrates that they have too little blood of any kind as well as too much pronephros and a little less endothelium. An intriguing finding of our work is that Fgf and Wnt signaling are elevated throughout the ventral and lateral regions of the *spt* gastrula, and later at the posterior tip of the embryo, a result that correlates with our observations that mutant embryos have excess posterior mesoderm. However, Fgf signals not only promote

posterior identity (Amaya et al., 1991; Dessimoz et al., 2006; Draper et al., 2003; Dubrulle and Pourquié, 2002; Pownall et al., 1996), they also prevent the undifferentiated progenitors that reside in the tail from precociously differentiating (Diez del Corral et al., 2003; Olivera-Martinez et al., 2012; Olivera-Martinez and Storey, 2007). It has been proposed that *spt* mutant cells are trapped in a transient state of mesodermal differentiation (Griffin and Kimelman, 2002; Row et al., 2011). Our observation that Fgf activity is elevated in the mutant explains the more "tail-like" attributes of mutant cells, this we propose is responsible for the *spt* intermediate mesoderm defect.

Non-cell autonomous role of Tbx16 for trunk patterning

It is well established that the *spt* gene product, Tbx16, has cell autonomous roles both in specifying cell fate and properly locating cells during gastrulation (Ho and Kane, 1990; Rohde et al., 2004; Row et al., 2011). Likely this explains why attenuating Fgf8a activity had so little effect on rescuing trunk blood cells in the mutant for not only is the signal antagonist *spry2* not regulated properly in *spt* mutants (Fig. 7C), but the transcription factor *mespa* is significantly downregulated (Garnett et al., 2009). Both are critical for hematopoietic cell fate (García-Domínguez et al., 2011; Hart et al., 2007). Likely however, many of the other defects we observe in posterior patterning are non-cell autonomous. Other zebrafish T-box transcription factors have essential non-cell autonomous roles. Both Brachyury and Ntl promote tail identity during later gastrulation and somitogenesis by maintaining expression of *wnt8a* and *wnt3a* (Martin and Kimelman, 2008; Morley et al., 2009). What if Tbx16 has a similar non-cell autonomous role only in promoting trunk identity during gastrulation by attenuating expression of *fgf8a*? Not only is *fgf8a* expression elevated in *spt* mutants, but *ntl* expression is as well. Fgf and Ntl are thought to induce the expression of each other (Isaacs et al., 1994; Schulte-Merker and Smith, 1995). However, others have shown that this autoregulatory loop is restricted to the axial mesoderm (Martin and Kimelman, 2008), and that in the nonaxial mesoderm, Ntl is downstream of Fgf signaling (Draper et al., 2003; Griffin et al., 1998; Olivera-Martinez et al., 2012). By regulating Fgf8a, Tbx16 could perhaps control trunk versus tail identity via Fgf8a's action on Ntl and downstream canonical Wnts (Fig. 9A).

The *spt* fate map

While initial dorsal-ventral position of a progenitor in the early gastrula is important for later anterior-posterior position of its derivatives (Kimmel et al., 1990; Lee et al., 1994; Stainier et al., 1993; Ward et al., 2007; Warga et al., 2009; Warga and Kimmel, 1990; Warga and Nusslein-Volhard, 1999), this relationship only correlates broadly because initial animal-vegetal position is also important. For presumptive mesoderm, how far from the margin a cell is positioned at the onset of gastrulation determines when it enters the mesodermal layer. Generally cells that lie close to the margin enter the mesodermal layer earlier and eventually lie more anterior than cells positioned further away (Kimmel et al., 1990; Warga and Kimmel, 1990; Warga and Nusslein-Volhard, 1999). Although our results show that all blood and endothelium in *spt* mutants derives from more or less the same dorsal location (rather than head blood and endothelium deriving exclusively from the dorsal half of the gastrula and trunk blood and endothelium deriving exclusively from the ventral half of the gastrula) we also demonstrate that head blood and endothelium in the mutant tend to originate from clones that lie close to the margin whereas trunk blood and endothelium from clones farther away (Fig. 9B). This was observed for pronephros as well. Thus the majority of trunk intermediate mesoderm in the mutant originated from clones located closer than normal to the animal pole suggesting that the dorsal-ventral axis in the mutant is translated into the animal-vegetal axis with respect to the later anterior-posterior position of head and trunk.

However while the axes for head and trunk are reconfigured in *spt* mutants on the gastrula fate map, the axes for tail are magnified. Rather than deriving from only the most ventral marginal cells, tail derivatives in the mutant such as caudal fin mesenchyme and tail muscle instead derive from the whole ventral half of the gastrula and from more animal cells (Fig. 9B). Thus the tail field of mutants usurps completely what is normally the trunk territory of intermediate mesoderm for all but pronephros, as well as what is normally the trunk territory of muscle (Kimmel et al., 1990; Warga and Nusslein-Volhard, 1999). Perhaps this explains the absence of intermediate mesoderm tissue most posteriorly in mutant embryos (Fig 3B–D). Because many of the cells in the wild-type trunk gastrula field normally incorporate into the tailbud temporarily as the trunk of the embryo is becoming organized (Kanki and Ho, 1997), it is possible that the *spt* tailbud does not contribute cells to the trunk unless they have pronephric fate, alternatively trunk cells that do not transit through the tailbud may have a greater tendency to become pronephros in *spt* mutants.

Fgf8 patterning of the intermediate mesoderm

Formation of the posterior of the zebrafish embryo is a continuum of cells being added to the trunk region during gastrulation and to the trunk and tail region during tailbud formation and elongation (Kanki and Ho, 1997; Kimmel et al., 1990; Warga and Kimmel, 1990). During this process, mesoderm cells express a series of genes and undergo a progression of cell behaviors associated with their differentiation state (Amacher et al., 2002; Goering et al., 2003; Griffin and Kimelman, 2002; Kanki and Ho, 1997; Row et al., 2011; Warga and Kimmel, 1990). Evidence suggests that *spt* mutant cells initiate the program of mesodermal differentiation, but fail to complete it because they persist in expressing genes and cell behaviors that should be transient (Griffin and Kimelman, 2002; Row et al., 2011) and this has been proposed to be why dorsal and lateral mesodermal cells in the mutant adopt cell behaviors reminiscent of cells on the more ventral side of the wild-type gastrula (Ho and Kane, 1990; Kimmel et al., 1989; Warga and Nusslein-volhard, 1998), as well as why trunk progenitors stay in the tailbud during somite stages (Griffin and Kimelman, 2002). It should be noted however, that this block in differentiation must not be permanent because eventually many of the dislocated mutant cells in the tail differentiate, sometimes as inappropriate fates given their beginning location (Kimmel et al., 1989). Thus while Tbx16 is not required for cells to initiate the differentiation program, it is necessary afterwards to repress some factor involved in keeping cells in an intermediate state of differentiation at least temporarily. Fgf8 signals are known to posteriorize, but some of this ability is due to its activity suppressing terminal differentiation of a relatively small pool of stem cell progenitors from which much of the posterior body is derived from (Diez del Corral et al., 2003; Kanki and Ho, 1997; Olivera-Martinez et al., 2012; Olivera-Martinez and Storey, 2007; Woo and Fraser, 1997). Our results indicate that Fgf8a is the factor that Tbx16 represses, likely indirectly as Tbx16 appears to act mainly as a transcriptional activator (Conlon et al., 122; Horb and Thomsen, 1997) and a likely intermediary target is the *mixer*-like transcription factor *bon* which microarray results (Garnett et al., 2009) indicate is downregulated 1.5-fold in *spt* mutants and whose *Xenopus* ortholog is known to regulate levels and/or durations of Fgf8 signals (Collins et al., 2010). Not only is *fgf8a* more highly expressed in *spt* mutants, but also where the least amount of transcripts occur correlates to where in the gastrula trunk intermediate mesoderm derives excluding pronephros (Fig. 9B). In wildtype, trunk blood and endothelium are biased to the ventral side of the gastrula, whereas *fgf8a* expression is biased to the dorsal side. In *spt* mutants, these biases are reversed, and tail derivatives such as caudal fin mesenchyme and tail muscle now derive from what in wildtype is the trunk domain. Likewise, trunk intermediate mesoderm in the mutant maps closer to the animal pole in accord with there being more *fgf8a* expression at the margin.

Perhaps the reallocation of intermediate mesoderm tissues in *spt* mutants simply results from excess Fgf8a posteriorizing the mesoderm causing presumptive trunk cells to acquire a tail fate. In zebrafish, blood only forms from mesoderm specified with the correct anterior-posterior identity, whereas this seems not so for pronephros or endothelium (Davidson et al., 2003; Wingert et al., 2007). This would be in keeping with our results that no Fgf8a and excessive Fgf8a appear to be deleterious for blood, as well the observation that *cdx4* and *cdx1a* are more highly expressed in the *spt* mutant (Fig. 6D, E). For *cdx* transcription factors, which convey anterior-posterior cell identity along the axis via regulation of the *hox* genes, are the targets of Fgf signaling (reviewed in: (Lohnes, 2003). Nevertheless, posterior identity must influence pronephric fate for as our results show the two are positively linked. Moreover, in both zebrafish and mouse, genetically attenuating Fgf8 activity not only results in less tail mesoderm, but also fewer kidney cells (Draper et al., 2003; Grieshammer et al., 2005; Perantoni et al., 2005).

There may however be another reason for the causal relationship between Fgf8a activity and pronephric fate. Clonal analysis in the zebrafish indicates that kidney identity is established well before blood and endothelial identity (Vogeli et al., 2006; Warga et al., 2009) and as intermediate mesoderm tissue becomes evident molecularly in the zebrafish, it expresses a series of genes that indicate all cells initially have the capacity to become kidney (reviewed in: (Davidson and Zon, 2004). It has been shown that Fgf8a function maintains expression of *pax2a* (one of the earliest kidney genes) in the midbrain-hindbrain boundary, another area in the embryo where *pax2a* is expressed (Reifers et al., 1998). Moreover, Fgfs suppress precocious blood differentiation (Bart nek et al., 2002; Colas et al., 2008; Walmsley et al., 2008; Willey et al., 2006). Perhaps by keeping cells in a kidney program and preventing cells from beginning a blood or endothelial program of development, Fgf8a holds cells in the less differentiated kidney state (like a tail stem cell progenitor). While blood cell fate seems exquisitely sensitive to Fgf8a activity in our experiments, possibly explaining why blood genes activate later than endothelial genes, macrophages are largely unaffected in *spt* mutants. This is likely because on the dorsal side of the gastrula, cells normally are exposed to much more Fgf8a. The advantage of Fgf8a delaying intermediate mesoderm cells from initiating a blood or endothelial differentiation pathway may be to not only create enough cells, but allow morphogenetic events to occur that bring these cells in proximity to new sources of inducing signals, for example trunk paraxial mesoderm which eventually is closely apposed to prospective red blood and crucial for its development (Rohde et al., 2004).

Sequence similarity indicates that zebrafish *tbx16* is an ortholog of chicken *Tbx6L*, and *Xenopus Xombie* (also known as *Antipodean*, *VegT*, and *Brat*) (Ruvinsky et al., 1998) and although there is no true mammalian ortholog, there is a high degree of similarity in expression and aspects of function between zebrafish *tbx16* and mouse *Tbx6* (Wardle and Papaioannou, 2008). Thus it will of interest to determine if a similar link exists between the Fgf8 signaling pathway and other vertebrate *tbx6* subfamily members in the formation of posterior mesoderm and the patterning of intermediate mesoderm.

Supplementary Material

Refer to Web version on PubMed Central for supplementary material.

Acknowledgments

References

Agathon A, Thisse C, Thisse B. The molecular nature of the zebrafish tail organizer. Nature. 2003; 424:448–452. [PubMed: 12879074]

Amacher SL, Draper BW, Summers BR, Kimmel CB. The zebrafish T-box genes *no tail* and *spadetail* are required for development of trunk and tail mesoderm and medial floor plate. Development. 2002; 129:3311–3323. [PubMed: 12091302]

Amaya E, Musci TJ, Kirschner MW. Expression of a dominant negative mutant of the FGF receptor disrupts mesoderm formation in Xenopus embryos. Cell. 1991; 66:257–270. [PubMed: 1649700]

Amin N, Vincan E. The Wnt signaling pathways and cell adhesion. Front Biosci. 2012; 17:784–804.

Araki I, Brand M. Morpholino-induced knockdown of fgf8 efficiently phenocopies the acerebellar (ace) phenotype. Genesis. 2001; 30:157–159. [PubMed: 11477697]

Auleha A, Pourquié O. Signaling gradients during paraxial mesoderm development. Cold Spring Harb Perspect Biol. 2010; 2:a000869. [PubMed: 20182616]

Baron MH, Fraser ST. The specification of early hematopoiesis in the mammal. Curr Opin Hematol. 2005; 12:217–221. [PubMed: 15867578]

Bart nek P, Pajer P, Karafiát V, Blendinger G, Dvorák M, Zenke M. bFGF signaling and v-Myb cooperate in sustained growth of primitive erythroid progenitors. Oncogene. 2002; 21:400–410. [PubMed: 11821952]

Begemann G, Schilling T, Rauch GJ, Geisler R, Ingham PW. The zebrafish neckless mutation reveals a requirement for raldh2 in mesodermal signals that pattern the hindbrain. Development. 2001; 128:3081–3094. [PubMed: 11688558]

Bennett CM, Kanki JP, Rhodes J, Liu TX, Paw BH, Kieran MW, Langenau DM, Delahaye-Brown A, Zon LI, Fleming MD, Look AT. Myelopoiesis in the zebrafish, *Danio rerio*. Blood. 2001; 98:643–651. [PubMed: 11468162]

Brownlie A, Hersey C, Oates AC, Paw BH, Falick AM, Witkowska HE, Flint J, Higgs D, Jessen J, Bahary N, Zhu H, Lin S, Zon LI. Characterization of embryonic globin genes of the zebrafish. Dev Biol. 2003; 255:48–61. [PubMed: 12618133]

Chappell JC, Bautch VL. Vascular development: genetic mechanisms and links to vascular disease. Curr Top Dev Biol. 2010; 90:43–72. [PubMed: 20691847]

Colas A, Cartry J, Buisson I, Umbhauer M, Smith JC, Riou JF. Mix. 1/2-dependent control of FGF availability during gastrulation is essential for pronephros development in *Xenopus*. Dev Biol. 2008; 320:351–365. [PubMed: 18614163]

Collins RT, Linker C, Lewis J. MAZe: a tool for mosaic analysis of gene function in zebrafish. Nat Methods. 2010; 7:219–223. [PubMed: 20139970]

Conlon FL, Sedgwick SG, Weston KM, Smith JC. Inhibition of Xbra transcription activation causes defects in mesodermal patterning and reveals autoregulation of Xbra in dorsal mesoderm. Development. 122:2427–2435. 122. [PubMed: 8756288]

Davidson AJ, Ernst P, Wang Y, Dekens MP, Kingsley PD, Palis J, Korsmeyer SJ, Daley GQ, Zon LI. cdx4 mutants fail to specify blood progenitors and can be rescued by multiple hox genes. Nature. 2003; 425:300–306. [PubMed: 13679919]

Davidson AJ, Zon LI. The 'definitive' (and 'primitive') guide to zebrafish hematopoiesis. Oncogene. 2004; 23:7233–7246. [PubMed: 15378083]

Davidson AJ, Zon LI. The caudal-related homeobox genes *cdx1a* and *cdx4* act redundantly to regulate hox gene expression and the formation of putative hematopoietic stem cells during zebrafish embryogenesis. Dev Biol. 2006; 292:506–518. [PubMed: 16457800]

Delarue M, Johnson KE, Boucaut JC. Superficial cells in the early gastrula of *Rana pipiens* contribute to mesodermal derivatives. Dev Biol. 1994; 165:702–715. [PubMed: 7958431]

Dessimoz J, Opoka R, Kordich JJ, Grapin-Botton A, Wells JM. FGF signaling is necessary for establishing gut tube domains along the anterior-posterior axis in vivo. Mech Dev. 2006; 123:42–55. [PubMed: 16326079]

Detrich, HWr; Kieran, MW.; Chan, FY.; Barone, LM.; Yee, K.; Rundstadler, JA.; Pratt, SJ.; Ransom, D.; Zon, LI. Intraembryonic hematopoietic cell migration during vertebrate development. Proc Natl Acad Sci. 1995; 92:10713–10717. [PubMed: 7479870]

Diez del Corral R, Olivera-Martinez I, Goriely A, Gale E, Maden M, Storey K. Opposing FGF and retinoid pathways control ventral neural pattern, neuronal differentiation, and segmentation during body axis extension. Neuron. 2003; 40:65–79. [PubMed: 14527434]

Diez del Corral R, Storey KG. Opposing FGF and retinoid pathways: a signalling switch that controls differentiation and patterning onset in the extending vertebrate body axis. BioEssays. 2004; 26:857–869. [PubMed: 15273988]

Draper BW, Stock DW, Kimmel CB. Zebrafish fgf24 functions with fgf8 to promote posterior mesodermal development. Development. 2003; 130:4639–4654. [PubMed: 12925590]

Dressler GR. The cellular basis of kidney development. Annu Rev Cell Dev Biol. 2006; 22:509–529. [PubMed: 16822174]

Dressler GR. Advances in early kidney specification, development and patterning. Development. 2009; 136:3863–3874. [PubMed: 19906853]

Drummond I. Making a zebrafish kidney: a tale of two tubes. Trends Cell Biol. 2003; 13:357–365. [PubMed: 12837606]

Dubrulle J, Pourquié O. From head to tail: links between the segmentation clock and antero-posterior patterning of the embryo. Curr Opin Genet Dev. 2002; 12:519–523. [PubMed: 12200156]

Dubrulle J, Pourquié O. fgf8 mRNA decay establishes a gradient that couples axial elongation to patterning in the vertebrate embryo. Nature. 2004; 427:419–422. [PubMed: 14749824]

Duester G. Retinoic acid synthesis and signaling during early organogenesis. Cell. 2008; 134:921–931. [PubMed: 18805086]

Fürthauer M, Lin W, Ang SL, Thisse B, Thisse C. Sef is a feedback-induced antagonist of Ras/MAPK-mediated FGF signalling. Nat Cell Biol. 2002; 4:170–174. [PubMed: 11802165]

Fürthauer M, Reifers F, Brand M, Thisse B, Thisse C. sprouty4 acts in vivo as a feedback-induced antagonist of FGF signaling in zebrafish. Development. 2001; 128:2175–2186. [PubMed: 11493538]

Fürthauer M, Thisse C, Thisse B. A role for FGF-8 in the dorsoventral patterning of the zebrafish gastrula. Development. 1997; 124:4253–4264. [PubMed: 9334274]

Fürthauer M, Van Celst J, Thisse C, Thisse B. Fgf signalling controls the dorsoventral patterning of the zebrafish embryo. Development. 2004; 131:2853–2864. [PubMed: 15151985]

García-Domínguez CA, Martínez N, Gragera T, Pérez-Rodríguez A, Retana D, León G, Sánchez A, Oliva JL, Pérez-Sala D, Rojas JM. Sprouty2 and Spred1–2 proteins inhibit the activation of the ERK pathway elicited by cyclopentenone prostanoids. PLoS One. 2011; 6:e16787. [PubMed: 21364986]

Garnett AT, Han TM, Gilchrist MJ, Smith JC, Eisen MB, FCW, Amacher SL. Identification of direct T-box target genes in the developing zebrafish mesoderm. Development. 2009; 136:749–760. [PubMed: 19158186]

Gibert Y, Gajewski A, Meyer A, Begemann G. Induction and prepatterning of the zebrafish pectoral fin bud requires axial retinoic acid signaling. Development. 2006; 133:2649–2659. [PubMed: 16774994]

Goering LM, Hoshijima K, Hug B, Bisgrove B, Kispert A, Grunwald D. An interacting network of T-box genes directs gene expression and fate in the zebrafish mesoderm. Proc Natl Acad Sci U S A. 2003; 100:9410–9415. [PubMed: 12883008]

Grieshammer U, Cebrián C, Ilagan R, Meyers E, Herzlinger D, Martin GR. FGF8 is required for cell survival at distinct stages of nephrogenesis and for regulation of gene expression in nascent nephrons. Development. 2005; 132:3847–3857. [PubMed: 16049112]

Griffin K, Patient R, Holder N. Analysis of FGF function in normal and no tail zebrafish embryos reveals separate mechanisms for formation of the trunk and the tail. Development. 1995; 121:2983–2994. [PubMed: 7555724]

Griffin KJ, Amacher SL, Kimmel CB, Kimelman D. Molecular identification of *spadetail*: regulation of zebrafish trunk and tail mesoderm formation by *T-box* genes. Development. 1998; 125:3379–3388. [PubMed: 9693141]

Griffin KJ, Kimelman D. One-Eyed Pinhead and Spadetail are essential for heart and somite formation. Nat Cell Biol. 2002; 4:821–825. [PubMed: 12360294]

Griffin KJ, Kimelman D. Interplay between FGF, one-eyed pinhead, and T-box transcription factors during zebrafish posterior development. Dev Biol. 2003; 264:456–466. [PubMed: 14651930]

Hacohen N, Kramer S, Sutherland D, Hiromi Y, Krasnow MA. sprouty encodes a novel antagonist of FGF signaling that patterns apical branching of the Drosophila airways. Cell. 1998; 92:253–263. [PubMed: 9458049]

Hans S, Christison J, Liu D, Westerfield M. Fgf-dependent otic induction requires competence provided by Foxi1 and Dlx3b. BMC Dev Biol. 2007; 7:5. [PubMed: 17239227]

Hans S, Westerfield M. Changes in retinoic acid signaling alter otic patterning. Development. 2007; 134:2449–2458. [PubMed: 17522161]

Hart DO, Raha T, Lawson ND, Green MR. Initiation of zebrafish haematopoiesis by the TATA-box-binding protein-related factor Trf3. Nature. 2007; 450:1082–1085. [PubMed: 18046332]

Hatada Y, Stern CD. A fate map of the epiblast of the early chick embryo. Development. 1994; 120:2879–2889. [PubMed: 7607078]

Heller N, Brändli AW. Xenopus Pax-2/5/8 orthologues: novel insights into Pax gene evolution and identification of Pax-8 as the earliest marker for otic and pronephric cell lineages. Dev Genet. 1999; 24:208–219. [PubMed: 10322629]

Herbomel P, Thisse B, Thisse C. Ontogeny and behaviour of early macrophages in the zebrafish embryo. Development. 1999; 126:3735–3745. [PubMed: 10433904]

Hill J, Clarke J, Vargesson N, Jowett T, Holder N. Exogenous retinoic acid causes specific alterations in the development of the midbrain and hindbrain of the zebrafish embryo including positional respecification of the Mauthner neuron. Mech Dev. 1995; 50:3–16. [PubMed: 7605750]

Ho RK, Kane DA. Cell-autonomous action of zebrafish *spt-1* mutation in specific mesodermal precursors. Nature. 1990; 348:728–730. [PubMed: 2259382]

Horb ME, Thomsen GH. A vegetally localized T-box transcription factor in Xenopus eggs specifies mesoderm and endoderm and is essential for embryonic mesoderm formation. Development. 1997; 124:1689–1698. [PubMed: 9165117]

Hug B, Walter V, Grunwald DJ. *tbx6*, a Brachyury-related gene expressed by ventral mesendodermal precursors in the zebrafish embryo. Devel Biol. 1997; 183:61–73. [PubMed: 9119115]

Isaacs HV, Pownall ME, Slack JM. eFGF regulates Xbra expression during Xenopus gastrulation. EMBO J. 1994; 13:4469–4481. [PubMed: 7925289]

Kanki JP, Ho RK. The development of the posterior body in zebrafish. Development. 1997; 124:881–893. [PubMed: 9043069]

Kelly GM, Greenstein P, Erezyilmaz DF, Moon RT. Zebrafish wnt8 and wnt8b share a common activity but are involved in distinct developmental pathways. Development. 1995; 121:1787–1799. [PubMed: 7600994]

Kessel M, Gruss P. Homeotic transformations of murine vertebrae and concomitant alteration of Hox codes induced by retinoic acid. Cell. 1991; 67:89–104. [PubMed: 1680565]

Kimelman D. Mesoderm induction: from caps to chips. Nat Rev Genet. 2006; 7:360–372. [PubMed: 16619051]

Kimmel CB, Kane DA, Walker C, Warga RM, Rothman MB. A mutation that changes cell movement and cell fate in the zebrafish embryo. Nature. 1989; 337:358–362. [PubMed: 2911386]

Kimmel CB, Warga RM, Schilling TF. Origin and organization of the zebrafish fate map. Development. 1990; 108:581–594. [PubMed: 2387237]

Krauss S, Johansen T, Korzh V, Fjose A. Expression of the zebrafish paired box gene pax[zf-b] during early neurogenesis. Development. 1991; 113:1193–1206. [PubMed: 1811936]

Kudoh T, Wilson SW, Dawid IB. Distinct roles for Fgf, Wnt and retinoic acid in posteriorizing the neural ectoderm. Development. 2002; 129:4335–4346. [PubMed: 12183385]

Lane MC, Sheets MD. Heading in a new direction: implications of the revised fate map for understanding *Xenopus laevis* development. Dev Biol. 2006; 296:12–28. [PubMed: 16750823]

Larson JD, Wadman SA, Chen E, Kerley L, Clark KJ, Eide M, Lippert S, Nasevicius A, Ekker SC, Hackett PB, Essner JJ. Expression of VE-cadherin in zebrafish embryos: a new tool to evaluate vascular development. Dev Dyn. 2004; 231:204–213. [PubMed: 15305301]

Le Guyader D, Redd MJ, Colucci-Guyon E, Murayama E, Kissa K, Briolat V, Mordelet E, Zapata A, Shinomiya H, Herbomel P. Origins and unconventional behavior of neutrophils in developing zebrafish. Blood. 2007; 111:132–141. [PubMed: 17875807]

Lee RK, Stainier DYR, Fishman MC. Cardiovascular development in the zebrafish. II Endocardial progenitors are sequestered within the heart field. Dev. 1994; 120:3361–3366.

Lekven AC, Thorpe CJ, Waxman JS, Moon RT. Zebrafish wnt8 encodes two wnt8 proteins on a bicistronic transcript and is required for mesoderm and neurectoderm patterning. Dev Cell. 2001; 1:103–114. [PubMed: 11703928]

Liao EC, Paw BH, Oates AC, Pratt SJ, Postlethwait JH, Zon LI. SCL/Tal-1 transcription factor acts downstream of *cloche* to specify hematopoietic and vascular progenitors in zebrafish. Genes Dev. 1998; 12:621–626. [PubMed: 9499398]

Lieschke GJ, Oates AC, Crowhurst MO, Ward AC, Layton JE. Morphologic and functional characterization of granulocytes and macrophages in embryonic and adult zebrafish. Blood. 2001; 98:3087–3096. [PubMed: 11698295]

Lieschke GJ, Oates AC, Paw BH, Thompson MA, Hall NE, Ward AC, Ho RK, Zon LI, Layton JE. Zebrafish *spi-1* (*pu.*1) marks a site of myeloid development independent of primitive erythropoiesis: implications for axial patterning. Dev Biol. 2002; 246:274–295. [PubMed: 12051816]

Lohnes D. The Cdx1 homeodomain protein: an integrator of posterior signaling in the mouse. Bioessays. 2003; 25:971–980. [PubMed: 14505364]

Ma M, Jiang YJ. Jagged2a-notch signaling mediates cell fate choice in the zebrafish pronephric duct. PLoS Genet. 2007; 3:e18. [PubMed: 17257056]

Marlow F, Gonzalez EM, Yin C, Rojo C, Solnica-Krezel L. No tail cooperates with non-canonical Wnt signaling to regulate posterior body morphogenesis in zebrafish. Development. 2004; 131:203–216. [PubMed: 14660439]

Martin BL, Kimelman D. Regulation of canonical Wnt signaling by Brachyury is essential for posterior mesoderm formation. Dev Cell. 2008; 15:121–133. [PubMed: 18606146]

Miller-Bertoglio V, Fisher S, Sanchez A, Mullins M, Halpern ME. Differential regulation of *chordin* expression domains in mutant zebrafish. Dev Biol. 1997; 192:537–550. [PubMed: 9441687]

Mohammadi M, McMahon G, Sun L, Tang C, Hirth P, Yeh BK, Hubbard SR, Schlessinger J. Structures of the tyrosine kinase domain of fibroblast growth factor receptor in complex with inhibitors. Science. 1997; 276:955–960. [PubMed: 9139660]

Morley RH, Lachani K, Keefe D, Gilchrist MJ, Flicek P, Smith JC, Wardle FC. A gene regulatory network directed by zebrafish No tail accounts for its roles in mesoderm formation. Proc Natl Acad Sci U S A. 2009; 106:3829–3834. [PubMed: 19225104]

Mueller RL, Huang C, Ho RK. Spatio-temporal regulation of Wnt and retinoic acid signaling by tbx16/ spadetail during zebrafish mesoderm differentiation. BMC Genomics. 2010; 11:492. [PubMed: 20828405]

Muyskens JB, Kimmel CB. Tbx16 cooperates with Wnt11 in assembling the zebrafish organizer. Mech Dev. 2007; 124:35–42. [PubMed: 17081734]

Naiche LA, Harrelson Z, Kelly RG, Papaioannou VE. T-box genes in vertebrate development. Annu Rev Genet. 2005; 39:219–239. [PubMed: 16285859]

Oates AC, Brownlie A, Pratt SJ, Irvine DV, Liao EC, Paw BH, Dorian KJ, Johnson SL, Postlethwait JH, Zon LI, Wilks AF. Gene duplication of zebrafish JAK2 homologs is accompanied by divergent embryonic expression patterns: only *jak2a* is expressed during erythropoiesis. Blood. 1999; 94:2622–2636. [PubMed: 10515866]

Oates AC, Pratt SJ, Vail B, Yan Yl, Ho RK, Johnson SL, Postlethwait JH, Zon LI. The zebrafish *klf* gene family. Blood. 2001; 98:1792–1801. [PubMed: 11535513]

Olivera-Martinez I, Harada H, Halley PA, Storey KG. Loss of FGF-Dependent Mesoderm Identity and Rise of Endogenous Retinoid Signalling Determine Cessation of Body Axis Elongation. PLoS Biol. 2012; 10:e1001415. [PubMed: 23118616]

Olivera-Martinez I, Storey KG. Wnt signals provide a timing mechanism for the FGF-retinoid differentiation switch during vertebrate body axis extension. Development. 2007; 134:2125–2135. [PubMed: 17507413]

Ota S, Tonou-Fujimori N, Yamasu K. The roles of the FGF signal in zebrafish embryos analyzed using constitutive activation and dominant-negative suppression of different FGF receptors. Mech Dev. 2009; 126:1–17. [PubMed: 19015027]

Perantoni AO, Timofeeva O, Naillat F, Richman C, Pajni-Underwood S, Wilson C, Vainio S, Dove LF, Lewandoski M. Inactivation of FGF8 in early mesoderm reveals an essential role in kidney development. Development. 2005; 132:3859–3871. [PubMed: 16049111]

Pfeffer PL, Gerster T, Lun K, Brand M, Busslinger M. Characterization of three novel members of the zebrafish Pax2/5/8 family: dependency of Pax5 and Pax8 expression on the Pax2.1 (*noi*) function. Development. 1998; 125:3063–3074. [PubMed: 9671580]

Phillips BT, Bolding K, Riley BB. Zebrafish fgf3 and fgf8 encode redundant functions required for otic placode induction. Dev Biol. 2001; 235:351–365. [PubMed: 11437442]

Poss KD, Shen J, Nechiporuk A, McMahon G, Thisse B, Thisse C, Keating MT. Roles for Fgf signaling during zebrafish fin regeneration. Dev Biol. 2000; 222:347–358. [PubMed: 10837124]

Pownall ME, Tucker AS, Slack JM, Isaacs HV. eFGF, Xcad3 and Hox genes form a molecular pathway that establishes the anteroposterior axis in Xenopus. Development. 1996; 122:3881–3892. [PubMed: 9012508]

Prince VE, Joly L, Ekker M, Ho RK. Zebrafish hox genes: genomic organization and modified colinear expression patterns in the trunk. Development. 1998; 125:407–420. [PubMed: 9425136]

Pyati UJ, Webb AE, Kimelman D. Transgenic zebrafish reveal stage-specific roles for Bmp signaling in ventral and posterior mesoderm development. Development. 2005; 132:2333–2343. [PubMed: 15829520]

Ramel MC, Buckles GR, Baker KD, Lekven AC. WNT8 and BMP2B co-regulate non-axial mesoderm patterning during zebrafish gastrulation. Dev Biol. 2005; 287:237–248. [PubMed: 16216234]

Rauch GJ, Hammerschmidt M, Blader P, Schauerte HE, Strähle U, Ingham PW, McMahon AP, Haffter P. Wnt5 is required for tail formation in the zebrafish embryo. Cold Spring Harb Symp Quant Biol. 1997; 62:227–234. [PubMed: 9598355]

Reifers F, Böhli H, Walsh EC, Crossley PH, Stainier DYR, Brand M. Fgf8 is mutated in zebrafish *acerebellar* (*ace*) mutants and is required for maintenance of midbrain-hindbrain boundary development and somitogenesis. Development. 1998; 125:2381–2395. [PubMed: 9609821]

Rohde LA, Oates AC, Ho RK. A crucial interaction between embryonic red blood cell progenitors and paraxial mesoderm revealed in *spadetail* embryos. Dev Cell. 2004; 7:1–20. [PubMed: 15239945]

Row RH, Maître JL, Martin BL, Stockinger P, Heisenberg CP, Kimelman D. Completion of the epithelial to mesenchymal transition in zebrafish mesoderm requires Spadetail. Dev Biol. 2011; 354:102–110. [PubMed: 21463614]

Ruvinsky I, Silver LM, Ho RK. Characterization of the zebrafish *tbx16* gene and evolution of the vertebrate T-box family. Dev Genes Evol. 1998; 208:94–99. [PubMed: 9569350]

Schier AF, Talbot WS. Molecular genetics of axis formation in zebrafish. Annu Rev Genet. 2005; 39:561–613. [PubMed: 16285872]

Schneider S, Steinbeisser H, Warga RM, Hausen P. Beta-catenin translocation into nuclei demarcates the dorsalizing centers in frog and fish embryos. Mech Dev. 1996; 57:191–198. [PubMed: 8843396]

Schulte-Merker S, Eeden FV, Halpern ME, Kimmel CB, Nüsslein-Volhard C. *no tail* (*ntl*) is the zebrafish homologue of the mouse *T* (*Brachyury*) gene. Development. 1994; 120:1009–1015. [PubMed: 7600949]

Schulte-Merker S, Smith JC. Mesoderm formation in response to Brachyury requires FGF signalling. Curr Biol. 1995; 5:62–67. [PubMed: 7535172]

Serluca F, Fishman MC. Pre-pattern in the pronephric kidney field of zebrafish. Development. 2001; 128:2233–2241. [PubMed: 11493543]

Skromne I, Thorsen D, Hale M, Prince VE, Ho RK. Repression of the hindbrain developmental program by Cdx factors is required for the specification of the vertebrate spinal cord. Development. 2007; 134:2147–2158. [PubMed: 17507415]

Stafford D, Prince VE. Retinoic acid signaling is required for a critical early step in zebrafish pancreatic development. Curr Biol. 2002; 12:1215–1220. [PubMed: 12176331]

Stainier DYR, Lee RK, Fishman MC. Cardiovascular development in the zebrafish: I. Myocardial fate map and heart tube formation. Development. 1993; 119:31–40. [PubMed: 8275863]

Stern CD, Charité J, Deschamps J, Duboule D, Durston AJ, Kmita M, Nicolas JF, Palmeirim I, Smith JC, Wolpert L. Head-tail patterning of the vertebrate embryo: one, two or many unresolved problems? Int J Dev Biol. 2006; 50:3–15. [PubMed: 16323073]

Sylvie J, Ellen C, Kris V. The role of Wnt in cell signaling and cell adhesion during early vertebrate development. Front Biosci. 2011; 17:2352–2366.

Thisse, B.; Pflumio, S.; Fürthauer, M.; Loppin, B.; Heyer, V.; Degrave, A.; Woehl, R.; Lux, A.; Steffan, T.; Charbonnier, XQ.; Thisse, C. Expression of the zebrafish genome during embryogenesis. 2001. http://zfin.org (NIH R01 RR15402)

Thisse C, Thisse B. High-resolution in situ hybridization to whole-mount zebrafish embryos. Nat Protoc. 2008; 3:59–69. [PubMed: 18193022]

Thompson MA, Ransom DG, Pratt SJ, MacLennan H, Kieran MW, Detrich HW, Vail B, Huber TL, Paw BH, Brownlie AJ, Oates AC, Fritz A, Gates MA, Amores A, Bahary N, Talbot WS, Her H, Beier DR, Postlethwait JH, Zon LI. The *cloche* and *spadetail* genes differentially affect hematopoiesis and vasculogenesis. Dev Biol. 1998; 197:248–269. [PubMed: 9630750]

Tsang M, Friesel R, Kudoh T, Dawid IB. Identification of Sef, a novel modulator of FGF signalling. Nat Cell Biol. 2002; 4:165–169. [PubMed: 11802164]

Ueno S, Weidinger G, Osugi T, Kohn AD, Golob JL, Pabon L, Reinecke H, Moon RT, Murry CE. Biphasic role for Wnt/beta-catenin signaling in cardiac specification in zebrafish and embryonic stem cells. Proc Natl Acad Sci U S A. 2007; 104:9685–9690. [PubMed: 17522258]

van Amerongen R, Nusse R. Towards an integrated view of Wnt signaling in development. Development. 2009; 136:3205–3214. [PubMed: 19736321]

Vogeli KM, Jin SW, Martin GR, Stainier DY. A common progenitor for haematopoietic and endothelial lineages in the zebrafish gastrula. Nature. 2006; 443:337–339. [PubMed: 16988712]

Walmsley M, Ciau-Uitz A, Patient R. Adult and embryonic blood and endothelium derive from distinct precursor populations which are differentially programmed by BMP in Xenopus. Development. 2002; 129:5683–5695. [PubMed: 12421708]

Walmsley M, Cleaver D, Patient R. Fibroblast growth factor controls the timing of Scl, Lmo2, and Runx1 expression during embryonic blood development. Blood. 2008; 111:1157–1166. [PubMed: 17942750]

Ward AB, Warga RM, Prince VE. Origin of the zebrafish endocrine and exocrine pancreas. Dev Dyn. 2007; 236:1558–1569. [PubMed: 17474119]

Wardle FC, Papaioannou VE. Teasing out T-box targets in early mesoderm. Curr Opin Genet Dev. 2008; 18:418–225. [PubMed: 18778771]

Warga RM, Kane DA, Ho RK. Fate mapping embryonic blood in zebrafish: multi- and unipotential lineages are segregated at gastrulation. Dev Cell. 2009; 16:744–755. [PubMed: 19460350]

Warga RM, Kimmel CB. Cell movements during epiboly and gastrulation in zebrafish. Development. 1990; 108:569–580. [PubMed: 2387236]

Warga RM, Nusslein-volhard C. spadetail-dependent cell compaction of the dorsal zebrafish blastula. Dev Biol (NY 1985). 1998; 203:116–121.

Warga RM, Nusslein-Volhard C. Origin and development of the zebrafish endoderm. Development. 1999; 126:827–838. [PubMed: 9895329]

Weinberg ES, Allende ML, Kelly CS, Abdelhamid A, Murakami T, Andermann P, Doerre OG, Grunwald DJ, Riggleman B. Developmental regulation of zebrafish *MyoD* in wildtype, *no tail*, and *spadetail* embryos. Development. 1995; 122:271–280. [PubMed: 8565839]

Widelitz R. Wnt signaling through canonical and non-canonical pathways: recent progress. Growth Factors. 2005; 23:111–116. [PubMed: 16019432]

Willey S, Ayuso-Sacido A, Zhang H, Fraser ST, Sahr KE, Adlam MJ, Kyba M, Daley GQ, Keller G, Baron MH. Acceleration of mesoderm development and expansion of hematopoietic progenitors in differentiating ES cells by the mouse Mix-like homeodomain transcription factor. Blood. 2006; 107:3122–3130. [PubMed: 16403910]

Wingert RA, Selleck R, Yu J, Song HD, Chen Z, Song A, Zhou Y, Thisse B, Thisse C, McMahon AP, Davidson AJ. The cdx genes and retinoic acid control the positioning and segmentation of the zebrafish pronephros. PLoS Genet. 2007; 3:1922–1938. [PubMed: 17953490]

Woo K, Fraser SE. Specification of the zebrafish nervous system by nonaxial signals. Science. 1997; 277:254–257. [PubMed: 9211857]

Yamamoto A, Amacher SL, Kim SH, Geissert D, Kimmel CB, De Robertis EM. Zebrafish *paraxial protocadherin* is a downstream target of *spadetail* involved in morphogenesis of gastrula mesoderm. Development. 1998; 125:3389–3397. [PubMed: 9693142]

Highlights

- *spadetail* (*tbx16*) mutants are deficient in <u>all</u> types of early blood.

- *spadetail* mutants have fewer endothelial cells and far more pronephric cells.

- Anterior mesoderm is transfating to a more posterior fate in the *spadetail* mutant

- Fgf signaling is upregulated in *spadetail* mutants.

- Fgfs both promote pronephric fate and repress blood and endothelial fate.
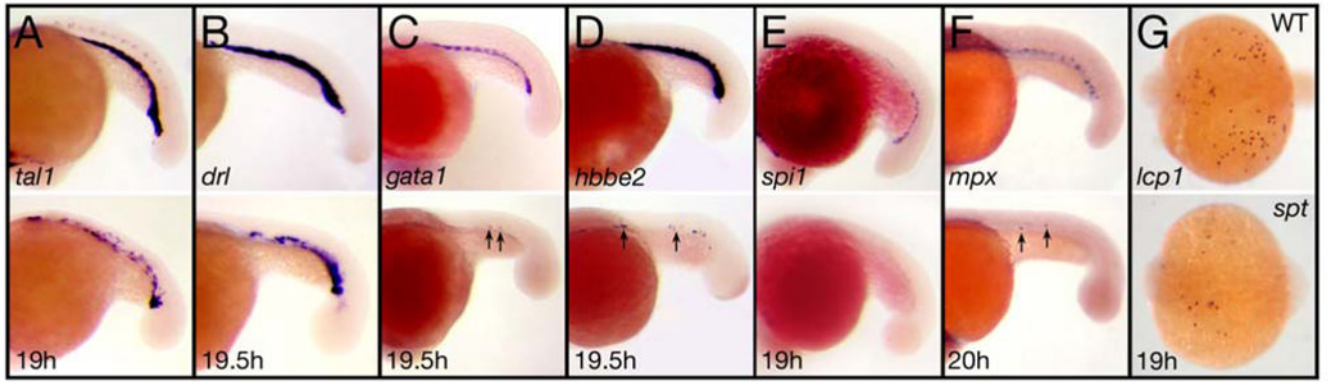
Figure 1. *spt* mutants have less of all types of blood

(A–F) Expression in the intermediate cell mass at 19 to 20 hours of: (A) *tal1* and (B) *drl* in all blood cells; (C) *gata1* and (D) *hbbe2* in red blood cells; (E) *spi1* in white blood cells; and (F) *mpx* in neutrophils. (G) *lcp* expression at 19 hours in macrophages derived from the head blood island.

Embryos are shown from a (A–F) left side view, or (G) dorsal view with anterior to the left. Arrows designate single cells.
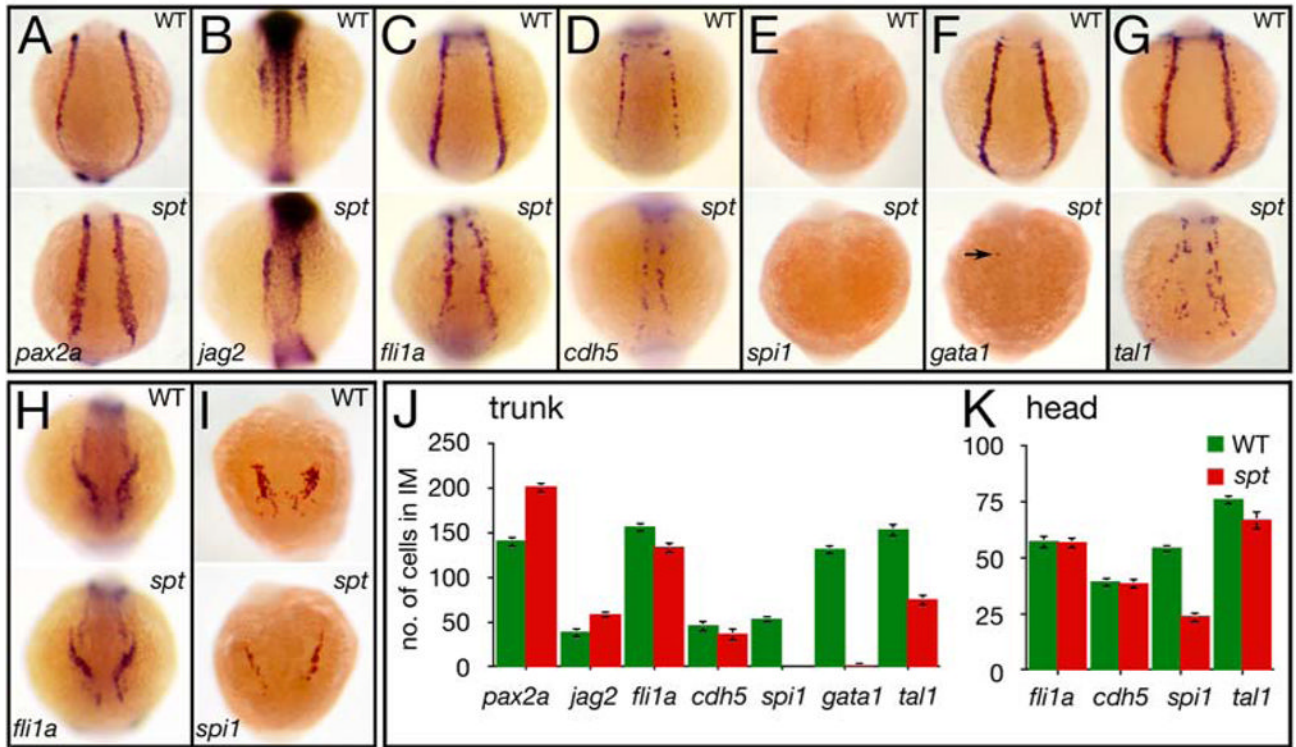
Figure 2. *spt* mutants possess more nephric precursors, but have fewer endothelial and hematopoietic precursors

(A–G) Expression in the trunk at 14.5 hours of: (A) *pax2a* and (B) *jag2*, in nephric cells; (C) *fli1a* and (D) *cdh5*, in endothelial cells; and (E) *spi1*, in white, (F) *gata1*, in red, and (G) *tal1*, in all blood cells (arrow designates a single cell).

(H–I) Expression in the head at 14.5 hours of: (H) *fli1a*, in endothelial cells; and (I) *spi1*, in macrophages.

(J–K) Quantification of intermediate mesoderm precursors for: (J) trunk, and (K) head. Graphs show the average number of cells per marker including standard error; 9 embryos for each category were counted.

Embryos are shown from a (A–G) posterior view, or (H–I) anterior view with dorsal to the top.
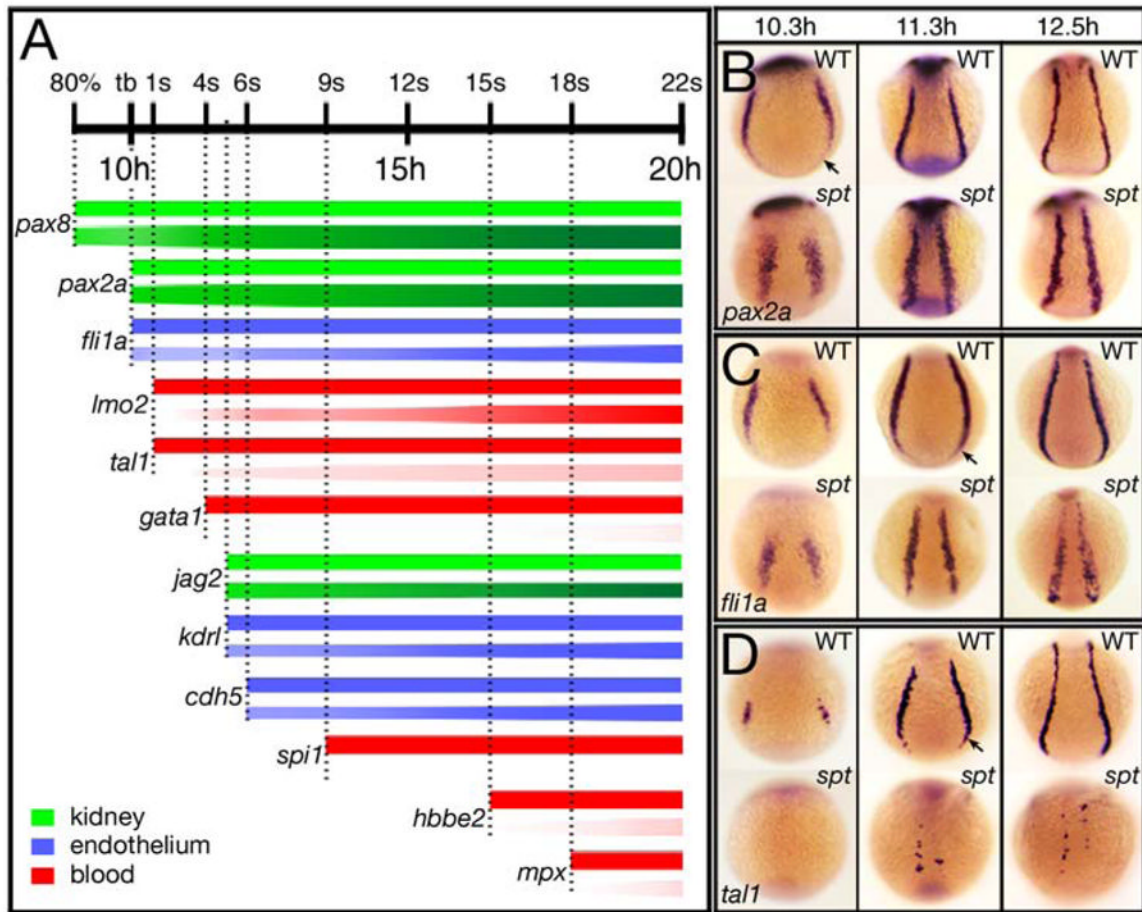
Figure 3. Spatiotemporal gene expression is altered in the intermediate mesoderm of *spt* mutants
(A) Temporal expression profiles of nephric (green), endothelial (blue) and hematopoietic (red) genes expressed in the trunk intermediate mesoderm. For each gene, the bar above symbolizes wild-type expression and the bar below mutant expression. Lightness or darkness of color for mutant denotes less or more cells. Vertical dotted lines denote onset of expression in wildtype. Examples of expression are shown in adjacent panels B–D and in Figs. 1, 2, 5 and Supplementary Fig. 2.
(B–D) Spatial pattern of trunk intermediate mesoderm genes: (B) *pax2a*, in nephric progenitors; (C) *fli1a*, in endothelial progenitors; and (D) *tal1*, in hematopoietic progenitors. Embryos are shown from a posterior view with dorsal to the top. Arrow designates portion missing in the mutant.
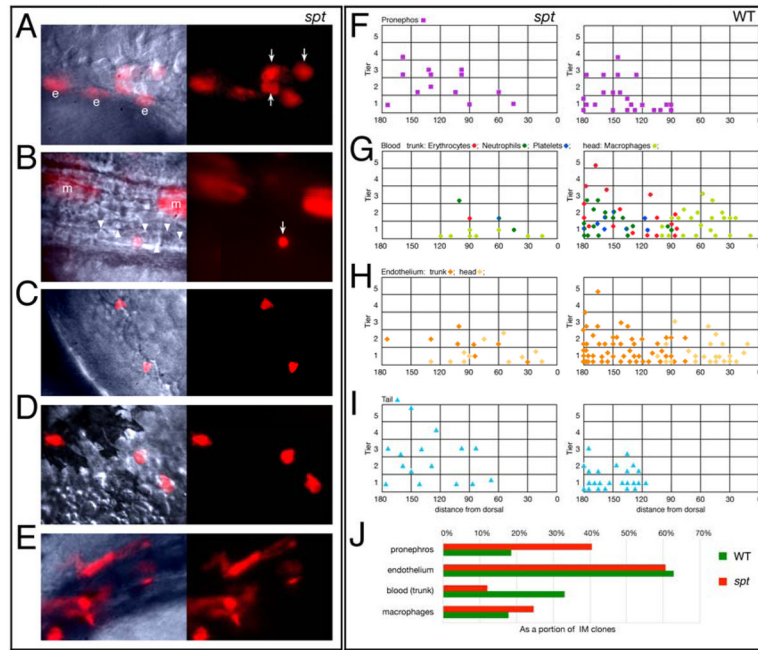
Figure 4. Trunk intermediate mesoderm and tail derivatives originate from more dorsal and animal locations in the *spt* mutant

(A–E) High magnification bright field and UV views of labeled cells in *spt* mutants at 24 to 36 hours: (A) Pronephric cells (arrows); (B) an erythrocyte (arrow), merged view shows neighboring unlabeled erythrocytes (arrowheads); (C) neutrophils; (D) macrophages; and (E) endothelial cells. All cells resembled their wild-type counterpart. Other labeled cells include hindgut endoderm (e) and muscle cells (m).

(F–J) Location of clones at 6 hours that gave rise to: (F) Pronephros; (G) Blood: trunk (erythrocytes, neutrophils and platelets) versus head (macrophages); (H) Endothelium: trunk versus head; and (I) Tail (caudal fin mesenchyme and tail muscle). For conventional presentation, clones are projected onto the left side even if they were on the right. Axes: y, distance from the blastoderm margin (zero) measured in cell tiers and x, distance from dorsal (zero) measured in degrees radian. For trunk blood, the color of the symbol indicates whether the clone gave rise only to erythrocytes (red), or also to neutrophils (green), platelets (blue) or both (green/blue).

(J) The percent of clones that gave rise to a specific derivative. The entire data set for intermediate mesoderm included 130 wild-type clones, and 33 mutant clones.
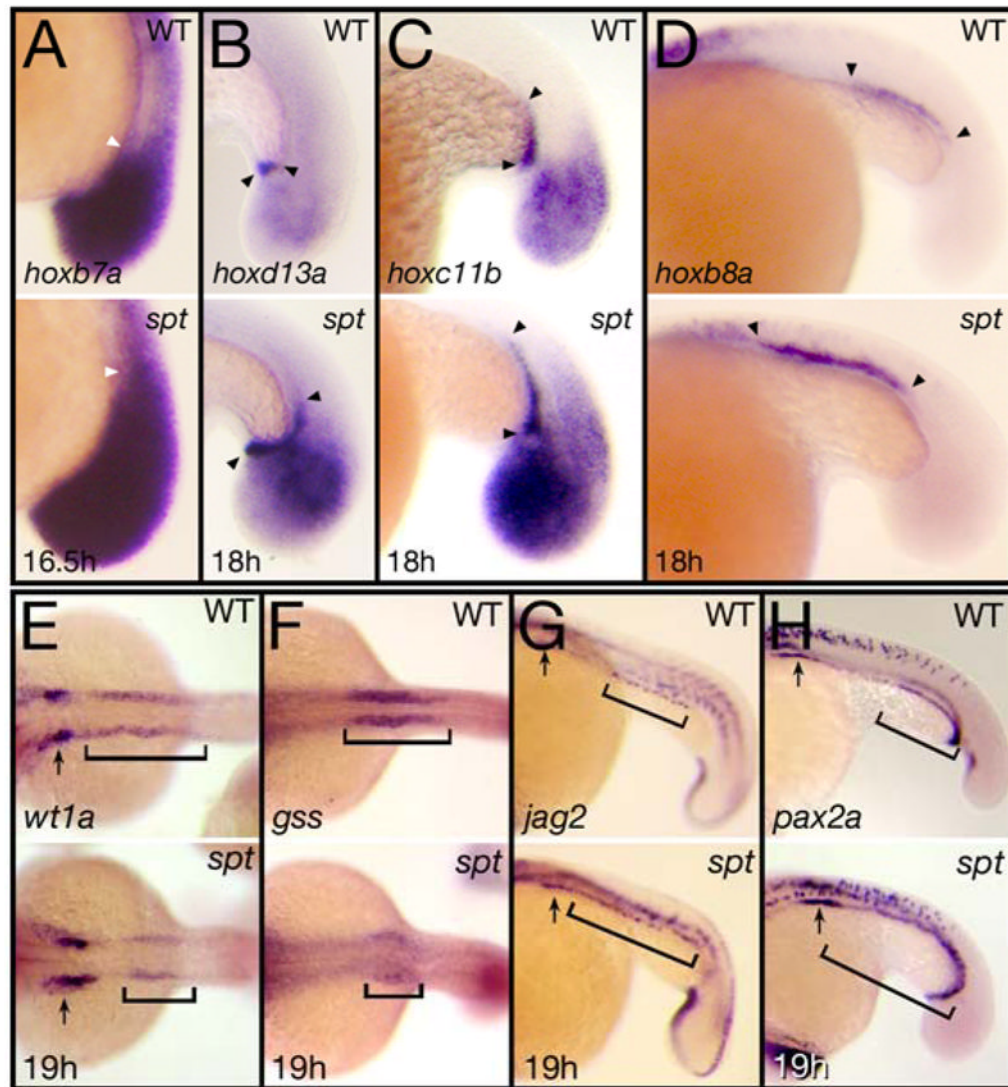
Figure 5. *spt* **mutants possess more posterior mesoderm**
(A) Expression at 16.5 hours of *hoxb6b*, arrowhead indicates the extent of anterior staining within the tailbud mesoderm. (B–D) Expression at 18 hours of: (B) *hoxd13a*, (C) *hoxc11b*, and (D) *hoxb8a*, arrowheads indicate extent of staining in the cloaca (B) or in the pronephros (C and D).
(E–I) Expression at 19 hours of: (E) *wt1a* and (F) *gss*, marking anterior segments and (G) *jag2* and (H) *pax2a*, marking posterior segments. Arrows indicate label in the most anterior nephric segment and brackets indicate regions that are altered.
Embryos are shown from a (A–D and G–H) left side view, or (E–F) dorsal view with anterior to the left.
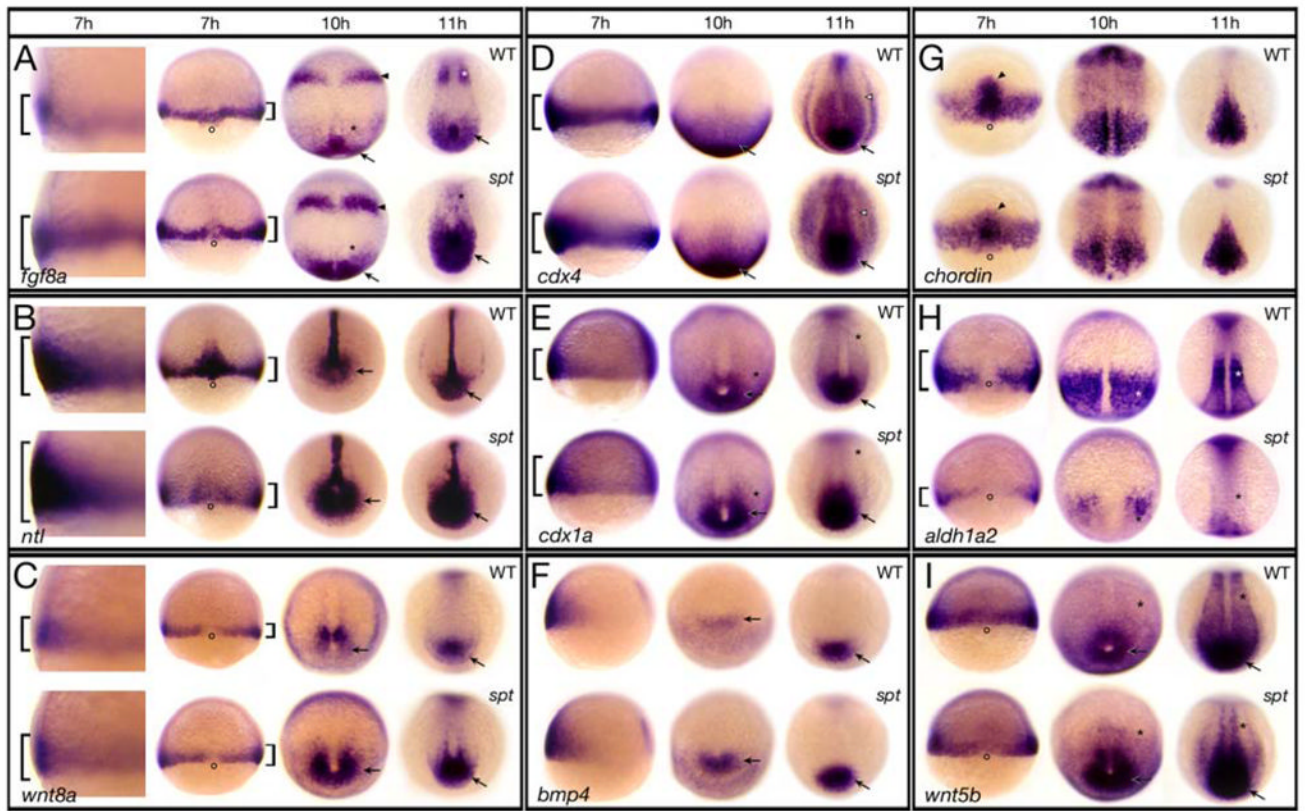
Figure 6. Components of the Fgf and Wnt pathway are more highly expressed in *spt* mutants
Expression of (A) *fgf8a*; (B) *ntl*; (C) *wnt8a*; (D) *cdx4*; (E) *cdx1a*; (F) *bmp4*; (G) *chordin*; (H) *aldh1a2*; and (I) *wnt5b* at: 7 hours, 10 hours and 11 hours.

Embryos at 7 hours are shown in (A–C) a high magnification left side view and a low magnification dorsal view, (D–F) a left side view, and (G–I) a dorsal view. Older embryos are all shown in a dorsal posterior view.

Designations (7 hours): brackets, more or less expression; open circles, dorsal side; arrowhead, prechordal plate; (later stages): arrow, more expression in the posterior region and tailbud; asterisk, less expression in the paraxial mesoderm; arrowhead, more expression in the future midbrain-hindbrain boundary; open arrowhead, more expression in the intermediate mesoderm.
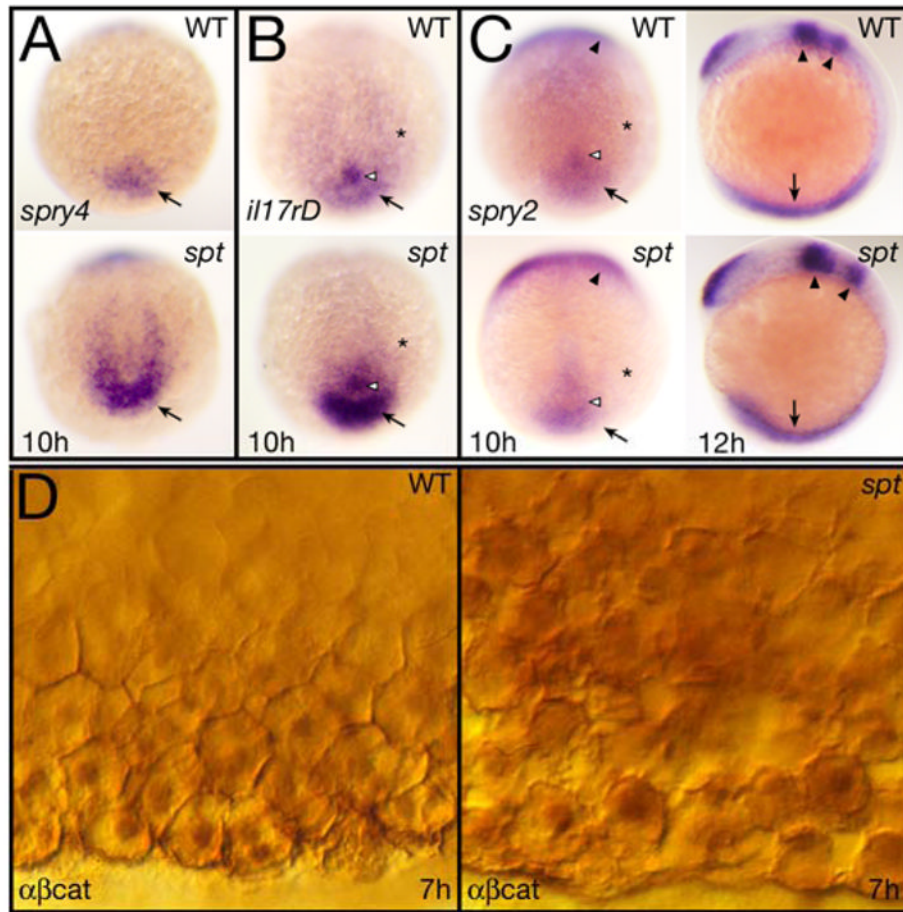
Figure 7. Fgf and Wnt signaling activity are elevated in *spt* mutants
(A–C) Expression at 10 and 12 hours of: (A) *spry4*, (B) *il17rD*, and (C) *spry2*.
All 10 hour embryos are shown in a dorsal posterior view, the 12 hour embryos in (C) are shown in left side view. Designations: arrow, tailbud (10 h) or posterior mesoderm (12 h); open arrowhead, Kupfer's vesicle; asterisk, paraxial mesoderm; and arrowheads, midbrain-hindbrain boundary region and rhombomere 4.
(D) Expression at 7 hours of β-catenin protein seen at high magnification in ventral marginal cells. Cells in the mutant (right), are not as cohesive with one another as in wildtype and make abnormal intercellular contacts and gaps. They also appear to have higher cytoplasmic and nuclear staining.
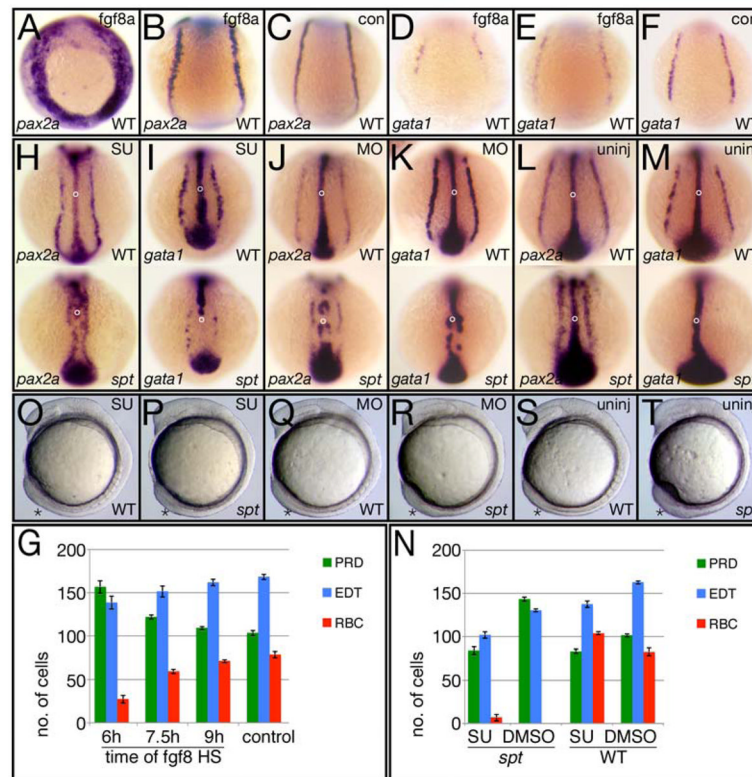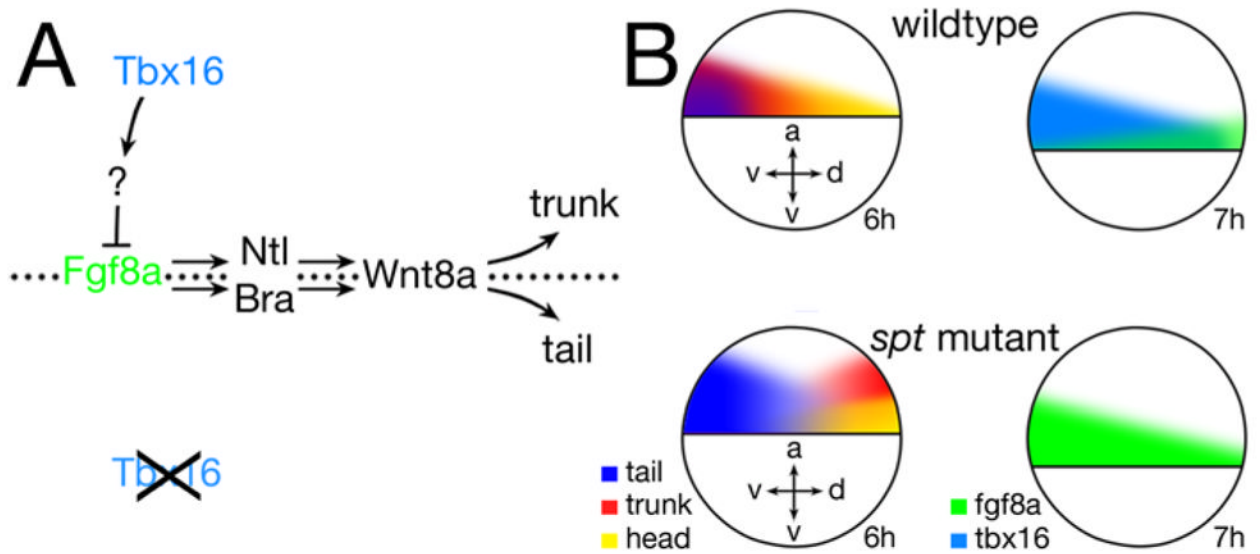
Figure 8. Altering Fgf8a signaling activity changes the balance of intermediate mesoderm-derived fates

(A–G) Overexpressing *fgf8a* by heat-shock effects individual intermediate mesoderm fates differently. (A–F) *in situ* analysis at 12 hours after heat shock of the transgene at 6 hours showing different examples of the phenotypes. Control siblings (con) not carrying the transgene, were also heat-shocked. *pax2a* expression identifies pronephric precursors (PRD), *gata1* expression identifies red blood precursors (BLD) and (not shown) *fli1a* expression identifies endothelial precursors (EDT). (G) Quantification of precursor cells at 12 hours after heat shock at 6, 7.5 or 9 hours. Graphs show the average number of cells per fate and the standard error.

(H–T) Inhibiting Fgf8a activity effects individual intermediate mesoderm fates in an opposite manner to overexpression. (H–M) *in situ* analysis at 12 hours of embryos exposed to Su5402 for one hour at 6 hours (H, I), injected at the 2 to 8-cell stage with the *fgf8a* morpholino (K, L) and their uninjected siblings (L, M). Embryos were also probed with *ntl* to monitor the effect on morphogenesis (open circle designates the notochord). Note that the tailbud marked by *ntl* expression is also smaller in all the SU5402 treated and *fgf8a* morphant embryos. (N) Quantification of precursor cells at 12 hours after exposure to SU5402 for one hour at 6 hours. (O–T) Live embryos depicting the tailbud phenotype after one hour exposure to Su5402 at 6 hours (O, P), or following injection of the *fgf8a* morpholino (Q, R) and their uninjected siblings (S, T).

Embryos are shown from a (A–F and H–M) dorsal posterior view, or (O–T) left side view; asterisk designates the tailbud.

Figure 9. Tbx16 regulates posterior body formation via regulation of Fgf8a

(A) The presence and absence of Tbx16 activity. Fgf8a signaling activity normally induces Ntl and Bra, which together act to maintain Wnt8a and Wnt3a signals thereby causing cells to persist in a progenitor stem cell state conducive to becoming tail. Tbx16, likely through an intermediary (?), represses Fgf8a production. Where there is no Fgf8a signal, Ntl and Bra are not induced and Wnt8a and Wnt3a signals are not maintained allowing mesodermal precursors to differentiate and become trunk.

(B) Comparison of the gastrula fate map for head, trunk and tail to *fgf8a* and *tbx16* transcript distribution in wildtype versus *spt* mutant. *fgf8a* expression is biased to the dorsal side in wildtype, whereas *tbx16* expression is biased to the ventral side. In *spt* mutants where there is no *tbx16* activity, *fgf8a* expression occupies the *tbx16* expression domain and tail fates expand into the trunk domain whereas trunk fates now derive dorsally and more animally, correlating to where the least amount of *fgf8a* expression occurs. Axes: dorsal-ventral (d-v), and animal vegetal (a-v).